ISSN 0919-9896

環境工学研究

No. 276

2009. 3. 19

1. ヒートアイランド対策としてのクールマテリアルについて　　マテオス・サンタモリス

社団法人　空気調和・衛生工学会近畿支部

SHASE Kinki Branchi, Japan

TEL 06(6612)8857
FAX 06(6613)7890

目　　　次

― 研 究 報 告 ―

開催日　平成21年3月19日（木）


HEAT ISLAND RESEARCH AT THE UNIVERSITY OF ATHENS
Mat Santamouris


Source : M. Santamouris : Heat Island Research in Europe - The State of the Art, J. Adv Build Energ Res, 2007
Heat Island is well documented in Europe. Studies have been performed in more than 30 cities using mobile and stationery measuring systems and devices.
76

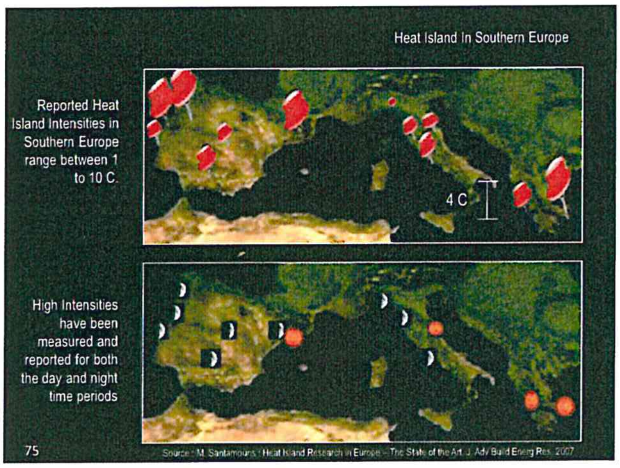
Heat Island In Southern Europe
Reported Heat Island Intensities in Southern Europe range between 1 to 10 C.
4 C
High Intensities have been measured and reported for both the day and night time periods
75
Source : M. Santamouris : Heat Island Research in Europe – The State of the Art, J. Adv Build Energ Res, 2007

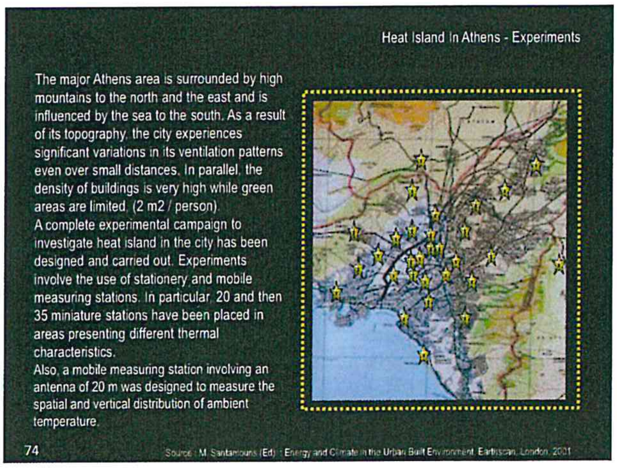
Heat Island In Athens - Experiments
The major Athens area is surrounded by high mountains to the north and the east and is influenced by the sea to the south. As a result of its topography, the city experiences significant variations in its ventilation patterns even over small distances. In parallel, the density of buildings is very high while green areas are limited. (2 m2 / person).
A complete experimental campaign to investigate heat island in the city has been designed and carried out. Experiments involve the use of stationery and mobile measuring stations. In particular, 20 and then 35 miniature stations have been placed in areas presenting different thermal characteristics.
Also, a mobile measuring station involving an antenna of 20 m was designed to measure the spatial and vertical distribution of ambient temperature.
74
Source : M. Santamouris (Ed) : Energy and Climate in the Urban Built Environment, Earthscan, London, 2001


Heat Island In Athens - Experiments
Stationery stations consists of miniature data loggers devices, which were used to measure air temperature and relative humidity. At each station white wooden boxes with lateral slots were constructed, similar to the Stevenson screen, in order to protect instruments from solar radiation and rain
The technical characteristics of the sensors and loggers used for the experiments are :
• Data storage capacity of 7600 readings, for the measurement of hourly values, the instrument can operate for approximately 300 days
• Temperature range -40 to 125 C
• Accuracy of the sensors : +- 0.2 C
All sensors were calibrated on a monthly basis in a temperature calibration oven, while in situ checks have been performed regularly using high accuracy sensors
73
Source : M. Santamouris (Ed) : Energy and Climate in the Urban Built Environment, Earthscan, London, 2001

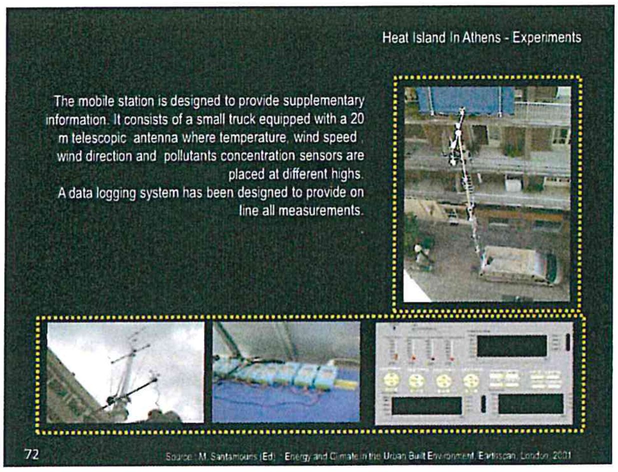
Heat Island In Athens - Experiments
The mobile station is designed to provide supplementary information. It consists of a small truck equipped with a 20 m telescopic antenna where temperature, wind speed, wind direction and pollutants concentration sensors are placed at different highs.
A data logging system has been designed to provide on line all measurements.
72
Source : M. Santamouris (Ed) : Energy and Climate in the Urban Built Environment, Earthscan, London, 2001

Heat Island In Athens - Experiments

In parallel, detailed measurements have been performed in 13 deep urban canyons, presenting different characteristics, to understand and evaluate the thermal and air flow phenomena. Ambient temperatures and wind speed and direction have been measured above and inside the canyons and in particular at various highs at the middle of the canyons and close to the facades.
Surface temperatures have been measured at the street level as well as on all facades at various highs.

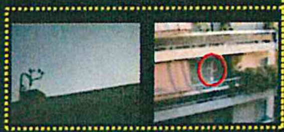

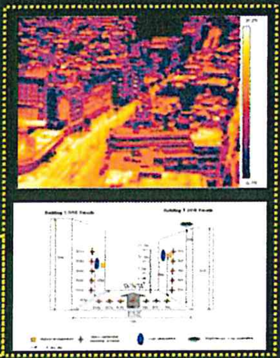

71

Source : M. Santamouris (Ed) : Energy and Climate in the Urban Built Environment, Earthscan, London, 2001

Characteristics of the Heat Island

Heat island development is a function of the synoptic climatic circulation in the lower troposphere. Heat island is mainly developed during the day time in the center and western part of Athens. These areas are characterised by high density and strong anthropogenic heat generation.

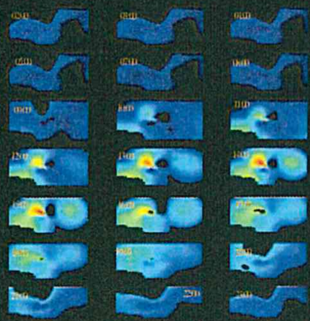

70

Source : M. Santamouris (Ed) : Energy and Climate in the Urban Built Environment, Earthscan, London, 2001

Characteristics of the Heat Island – Day Time - Summer

Temperature increase in the very central area may rich values up to 10 C. Heat island intensity is much lower to suburban areas and range between 2 to 6 C.
An almost linear relation between the absolute temperature in the urban station against the ΔT between the reference and the urban stations is observed. The higher the temperature in the urban station the higher the temperature difference

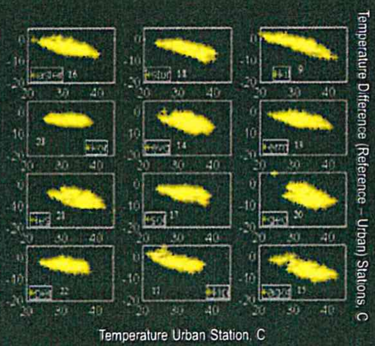

69

Source : M. Santamouris (Ed) : Energy and Climate in the Urban Built Environment, Earthscan, London, 2001

Characteristics of the Heat Island – Night Time - Summer

During the night period, heat island intensity varies between 2-5 C as a function of the station characteristics.
Urban green areas present 2-3 degrees lower temperature than the reference station.

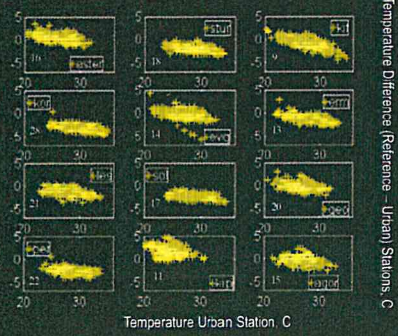

68

Source : M. Santamouris (Ed) : Energy and Climate in the Urban Built Environment, Earthscan, London, 2001

Characteristics of the Heat Island

To define the limits where the ranges of hourly temperatures fluctuate for urban and suburban stations, the observed ranges of absolute maximum and minimum air temperatures were estimated.
During the winter period the absolute minimum air temperature of urban stations are 2-3 C higher in comparison with the values of the suburban stations
During summer, the minimum of the absolute air maximum values in urban stations are 5-6 C greater than in the suburban stations while the maximum of the absolute maximum values exceed 2-5 C the respective maximum values of the suburban stations

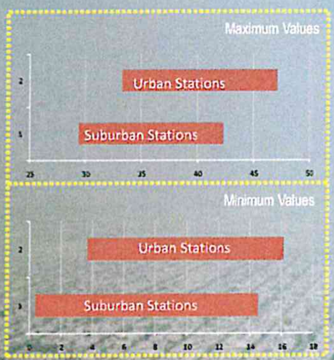

I. Livada, M. Santamouris, K. Niachou, N. Papanikolaou and G. Mihalakakou : "Determination of Places in the great Athens area where the heat island effect is observed", Theoretical Appl. Climatol., 71, 219-230, 2002.

67

Characteristics of the Heat Island

To analyse the phenomenon, all stations have been classified in urban and suburban using statistical criteria. It is found that there is a statistical significant correlation between the DH > 26 C and the number of hours above 26 C, for both the urban and suburban stations, thus the dynamics of the temperature variation in both groups present a statistically significant difference.
Also, the slope of the curves is statistically significant but not the difference of slopes, thus the dynamics of temperature evolution is different at the various temperature levels.

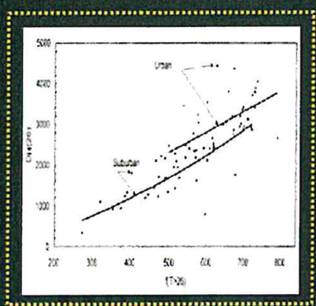

I. Livada, M. Santamouris, K. Niachou, N. Papanikolaou and G. Mihalakakou : "Determination of Places in the great Athens area where the heat island effect is observed", Theoretical Appl. Climatol., 71, 219-230, 2002.

66

Characteristics of the Heat Island

Same results have been found for the winter period. In parallel it is found that the elevation of both curves is statistically different, thus in urban places characterised with small values of existing air temperature values, the DH are greater than those of the suburban temperatures.
Using the Besson persistence coefficient it is calculated that the persistence of high temperatures is statistically significant, (T>26 C), for all stations. By applying the Mendenhall test it is found that persistence is mainly due to the stationarity of the weather conditions than because of the heat island effect

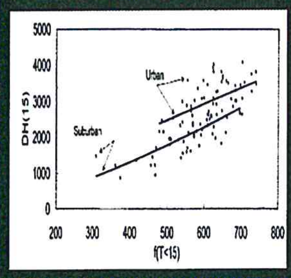

I. Livada, M. Santamouris, K. Niachou, N. Papanikolaou and G. Mihalakakou : 'Determination of Places in the great Athens area where the heat island effect is observed', Theoretical Appl. Climatol., 71, 219-230 2002.

65

Characteristics of the Heat Island

The effect of the synoptic-scale atmospheric circulation on the urban heat island phenomenon over Athens, was investigated and quantified. The 850-hPa atmospheric circulation was classified into eight a priori categories on a daily basis for a 2-yr period (1997-98), for all seasons, according to the form and relative position of the synoptic-scale features typically representing the complete range of the atmospheric circulation over the Mediterranean basin. The occurrence of the heat island phenomenon is then assessed relative to the synoptic categories (circulation to- environment approach).

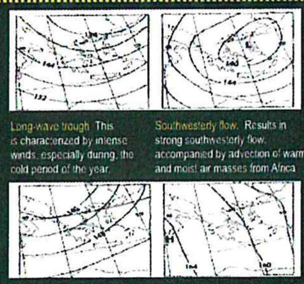

Long-wave trough. This is characterized by intense winds, especially during the cold period of the year.

Southwesterly flow. Results in strong southwesterly flow, accompanied by advection of warm and moist air masses from Africa

Northwesterly flow. This category is characterized by strong cold air advection from the north or northwest

Zonal flow. Westerly flow with considerably lower intensity in the warm period of the year.

G. Mihalakakou, H.A. Flocas, M. Santamouris and C.G. Helmis : 'Application of Neural Networks to the Simulation of the Heat Island over Athens, Greece, Using Synoptic Types as a Predictor', J. Applied Meteorology, 41,5,519-527,2002

64

Characteristics of the Heat Island

A multilayered neural network architecture, based on the Backpropagation algorithm, was selected for the estimation of the urban heat island intensity at each experimental site. Thus, a neural model was built separately for each of the 23 locations. The neural network model architecture consisted of one hidden layer of 20-25 so-called log-sigmoid neurons, followed by an output layer of one linear neuron. Learning was achieved using the backpropagation algorithm of Rumelhart et al, to train the network. An error goal of 0.5 was Selected, and the number of epochs varied between 2000 and 3000.

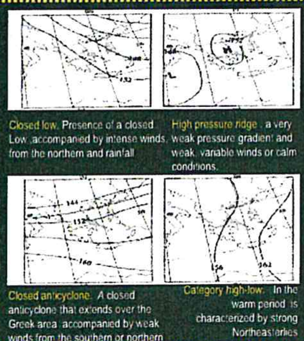

Closed low. Presence of a closed Low, accompanied by intense winds, and rainfall from the northern

High pressure ridge : a very weak pressure gradient and weak, variable winds or calm conditions.

Closed anticyclone. A closed anticyclone that extends over the Greek area, accompanied by weak winds from the southern or northern

Category high-low. In the warm period is characterized by strong Northeasterlies

G. Mihalakakou, H.A. Flocas, M. Santamouris and C.G. Helmis : 'Application of Neural Networks to the Simulation of the Heat Island over Athens, Greece, Using Synoptic Types as a Predictor', J. Applied Meteorology, 41,5,519-527,2002

63

Characteristics of the Heat Island

The input parameters of the neural models are

a. Synoptic-scale atmospheric circulation
b. Ambient air temperature measured at each station
c. Ambient air temperature measured at the reference station
d. Maximum daily values of total solar radiation
e. Mean daily values of wind speed

Training was performed using the input parameter values for the estimation of the heat island intensity for 500 days of 1997 and 1998. To test the results of the neural network, the model estimations were compared with the corresponding measurements of UHI intensity for the remaining 230 days of 1998 that compose the test dataset.

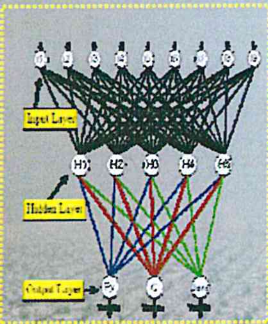

G. Mihalakakou, H.A. Flocas, N. Santamouris and C.G. Helmis : 'Application of Neural Networks to the Simulation of the Heat Island over Athens, Greece, Using Synoptic Types as a Predictor', J. Applied Meteorology, 41,5,519-537,2002

62

Characteristics of the Heat Island

Concerning the influence of each synoptic category on the UHI intensity, the neural network approach verified that anticyclonic categories High pressure ridge and Closed anticyclone, (weak winds), mostly favor the UHI. On the contrary, the northerly airflow (Northwesterly flow and Category high-low) appears to limit the phenomenon.
Good agreement is observed between the estimated and measured data for the whole set of testing data. 90 % of the relative error range between - 10% and 14%. The correlation coefficients vary from 0.86 to 0.94 while the root-mean-square errors range between 0.1 and 0.30 C.
To investigate the influence of atmospheric circulation on the UHI intensity, a neural network models were designed and trained using only the atmospheric circulation as input parameter.
It was demonstrated that synoptic conditions as the only input parameter contributes significantly to the UHI intensity estimation with correlation coefficients as high as 0.77

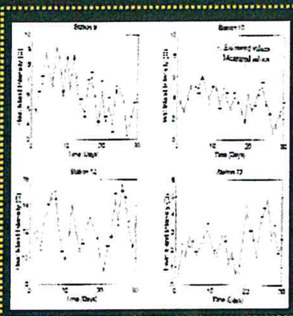

G. Mihalakakou, H.A. Flocas, M. Santamouris and C.G. Helmis : 'Application of Neural Networks to the Simulation of the Heat Island over Athens, Greece, Using Synoptic Types as a Predictor', J. Applied Meteorology, 41,5,519-527,2002

61

Energy Impact of the Heat Island

Iso-Cooling Degree Hours > 26 C at 1:00 during August

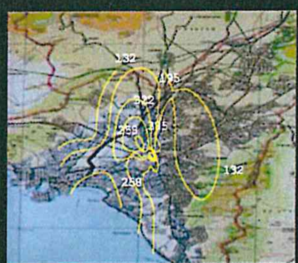

Iso-Cooling Degree Hours > 26 C at 13:00 during August

Calculation and mapping of cooling degree hours shows a strong stratification between the various areas of the city. Thus, a strong impact on the cooling energy demand has to be expected

M. Santamouris, N. Papanikolaou, I. Livada, I. Koronakis, C. Georgakis, A. Argiriou and D. N. Assimakopoulos : 'On the Impact of Urban Climate to the Energy Consumption of Buildings' Solar Energy, 70,3,201-216,2001

60

Energy Impact of the Heat Island

Using the measured temperatures in all stations detailed simulations have been carried out for a typical office building using TRNSYS. Simulations have been performed for a two years period and for a set point temperature of 27 C, and are compared against measurements collected in the building and it is found that the model is accurate.
It is found that monthly sensible cooling loads in the center of the city increases up to 130 % compared to the reference region. In parallel, cooling load in western Athens increases by 75 %.
Lower cooling loads are calculated in the coastal area where the impact of the sea breeze is important

M. Santamouris, N. Papanikolaou, I. Livada, I. Koronakis, C. Georgakis, A. Argiriou and D. N. Assimakopoulos : On the Impact of Urban Climate to the Energy Consumption of Buildings' Solar Energy, 70,3,201-216,2001

Energy Impact of the Heat Island

In parallel, using TRNSYS simulations for the same typical building, the peak electricity load for sensible cooling has been calculated for a two years period and for a set point temperature of 27 C.
It is found that peak electricity demand in the city center may increase up to 300 %, compared to the reference region while in western Athens, the relative increase is up to 200 %.
In parallel, it is calculated and measured that COP of room air conditioners decreases up to 25 % in the central Athens area

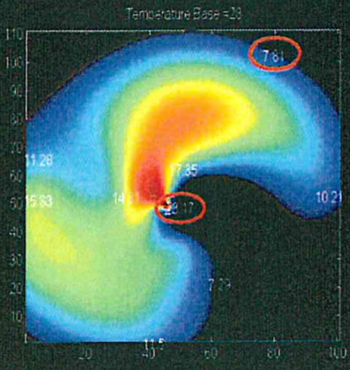

M. Santamouris, N. Papanikolaou, I. Livada, I. Koronakis, C. Georgakis, A. Argiriou and D. N. Assimakopoulos : On the Impact of Urban Climate to the Energy Consumption of Buildings' Solar Energy, 70,3,201-216,2001

Energy Impact of the Heat Island

Heating degree hours, (base 18,3 C), in the central Athens area are to about 30 % lower compared to the reference region.
As it concerns the possible reduction of the heating load because of the UHI, simulations have shown that there is a decrease in the central Athens area between 30 -50 %.

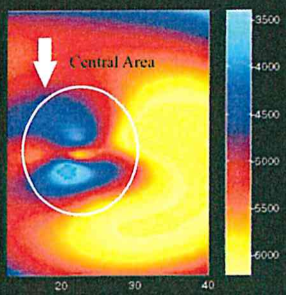

M. Santamouris, N. Papanikolaou, I. Livada, I. Koronakis, C. Georgakis, A. Argiriou and D. N. Assimakopoulos : On the Impact of Urban Climate to the Energy Consumption of Buildings' Solar Energy, 70,3,201-216,2001

Environmental Impact of the Heat Island

Using GIS information on the distribution and type of buildings in Athens, simulations have been performed using TRNSYS to calculate the additional electricity demand in Athens because of the presence of UHI. Then, the additional ecological footprint because of the UHI is calculated. It is found that it is equal to 1,5 times the actual size of the Municipality of Athens. Additional CO2 emissions are between 0.3-0.4 MT / year.

Year	1997	1998
Maximum potential Athens' heat island energy cost (kWh/m^2)	33.2	29.0
Maximum potential Total Athens' heat island energy cost (GWh)	1,540.5	1,345.6
Maximum potential CO_2 emissions (Mtn)	4,621	4,036
Maximum potential ecological footprint of the Athens' heat island (ha)	901,180	787,176

Year	1997	1998
Actual total Athens' heat island energy cost (GWh)	120.7	105.5
Actual potential CO_2 emissions (Mtn)	0.362	0.316
Actual ecological footprint of the Athens' heat island (ha)	70,562	61,714

M. Santamouris, K. Paraponiaris and G. Mihalakakou . Estimating the Ecological Footprint of the Heat Island effect over Athens, Greece Climate Change,(2007) 80,265-276.

Environmental Impact of the Heat Island

The impact of temperature on the tropospheric ozone concentration levels in the urban area of Athens has been investigated. Air temperature and ozone concentration data from several experimental stations in the greater Athens area were collected and used for performing linear correlations and temporal variation analysis. Furthermore, the analysis was enriched with a neural network method for achieving a more quantitative approach of the influence of temperature on the ozone concentration values over the greater Athens area. Ambient air temperature and NOx concentration values were mainly used as input parameters to the neural network models. The results showed that temperature is a predominant parameter, affecting considerably the ozone concentration values.

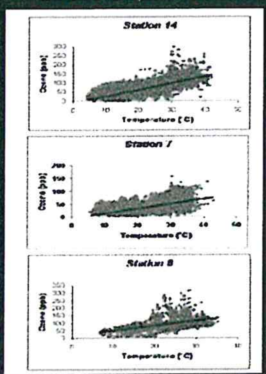

E Stathopoulou, G Mihalakakou, M Santamouris and H S Bagiorgas , Impact of Temperature on Tropospheric Ozone Concentration Levels in Urban Environments, J. of Earth System Science, In Press, 2008

Temporal Prediction of the Heat Island

Ambient temperature time series are non linear dynamic systems, are not functions having a normal sinusoidal or semi – sinusoidal characteristics, while do not present a not predictable full stochastic behavior. On the contrary are characterised by a dynamic chaotic behavior with an evident deterministic component.
Long term predictions are not possible in chaotic systems, as errors increase exponentially with time, however, predictions for short periods may be very accurate.
To quanify non linear dynamics, two parameters are used. The Dimension and the Lyapunov exponent of the attractor of the system. The dimension of the attractor is related to the degree of freedom of the system while positive Lyapunov exponents indicate the degree of information loss.

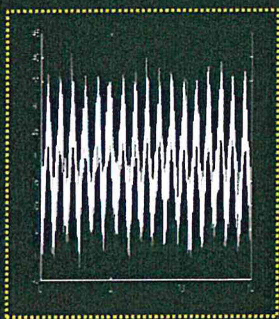

G. Mihalakakou, M. Santamouris, and D. Asimakopoulos : Modeling ambient air temperature time series using neural Networks J Geophysical Research, 103, D16, PP 19509-19517, 1998

Temporal Prediction of the Heat Island

A methodology has been developed to optimise a NN to predict future values of temperature time series. The following steps have been followed :

1. Reconstruction of the temperature time series using the method of time delays.
2. Calculation of the dimension D2 and of the maximum Lyapunov exponent.
3. Calculation of the scaling region
4. Calculation of the dimension m at which the correlation integral converges to D2
5. Definition of the number of inputs of the NN equal to the dimension m for which convergance is achieved.
6. Definition of the prediction time period

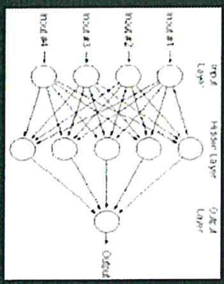

G. Mihalakakou, M. Santamouris, and D. Asimakopoulos : Modeling ambient air temperature time series using neural Networks. J Geophysical Research, 103, D16, P.P. 15509-15517, 1998

53

Temporal Prediction of the Heat Island

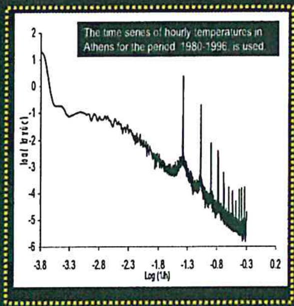

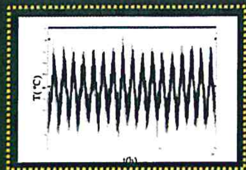

The temporal evolution of the hourly values of ambient temperature is determined by a deterministic component while low frequencies are observed in the power spectrum of the time series. The spectrum is not distinct, and despite the fact that the daily frequency and harmonics are evident, the form presented, is consistent with a continuous spectrum and thus a low dimension dynamic.

G. Mihalakakou, M. Santamouris, and D. Asimakopoulos : Modeling ambient air temperature time series using neural Networks. J Geophysical Research, 103, D16, P.P. 15509-15517, 1998

52

Temporal Prediction of the Heat Island

Maximum Lyapunov Exponent

The Lyapunov exponent is a measure of the rate of information loss during the evolution of the system. The maximun Lyapunov exponent , λmax, for the temperature time series has been calculated using the Wolf algorithm. A positive Lyapunov exponent is a strong indication of a the existence of a low dimesion chaos.

It is found that the maximum Lyapunov exponent is equal to λmax= 0.034 bits/h.

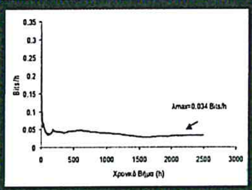

$$\lambda_i = \lim_{t \to \infty} \frac{1}{t} \log_2 \frac{\varepsilon_i(t)}{\varepsilon(0)}$$

G. Mihalakakou, M. Santamouris, and D. Asimakopoulos : Modeling ambient air temperature time series using neural Networks. J Geophysical Research, 103, D16, P.P. 15509-15517, 1998

51

Temporal Prediction of the Heat Island

Control: Data results from a linear stochastic procedure

Using the method of false data, it is found that the time series is not the result of a linear correlated

Control : Data results from a non linear deformation of a linear procedure

Using the method of false data it is found that the time series is not the result of a non linear deformation of a linear procedure.

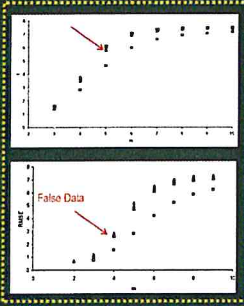

RMSE for real and false data as a function of the embedding dimension

G. Mihalakakou, M. Santamouris, and D. Asimakopoulos : Modeling ambient air temperature time series using neural Networks. J Geophysical Research, 103, D16, P.P. 15509-15517, 1998

50

Temporal Prediction of the Heat Island

The number of Inputs is defined by the dimension of saturation ,and the sampling from the time delay constant .

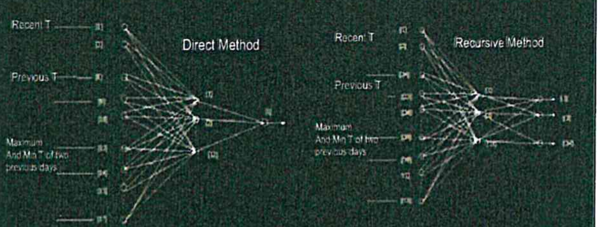

Direct Method

Input	Description	
1-8	T(t)	t=1,...,8
9-13	T(d,t+1)	d=(d-1),...,(d-5)
14-15	$T_{max}(d-1)$,$T_{min}(d-1)$	
16-17	$T_{max}(d-2)$, $T_{min}(d-2)$	
Output	**Description**	
1	T(d,t+1)	

Recursive Method

Input	Description	
1-24	T(d-1,t)	t=1,...,24
25-29	T(d,t)	d=d-2,...,d-6
30-31	$T_{max}(d-1)$,$T_{min}(d-1)$	d=d-1
32-33	$T_{max}(d-2)$, $T_{min}(d-2)$	d=d-2
Output	**Description**	
24	T(d,t)	t=1,24

G. Mihalakakou, M. Santamouris, and D. Asimakopoulos : Modeling ambient air temperature time series using neural Networks. J Geophysical Research, 103, D16, P.P. 15509-15517, 1998

49

Temporal Prediction of the Heat Island

One Step Prediction

The mean annual error for prediction of one time step has been calculated for using a) a sampling constant τ=1 (h), b) τ=8 . The mean annual error for both models is 2.6% and 2.8% respectively.

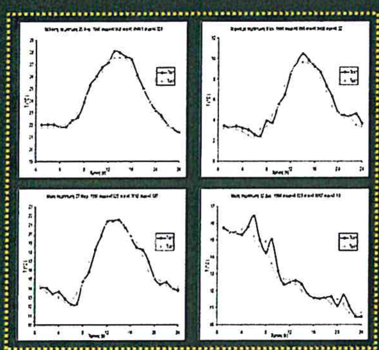

G. Mihalakakou, M. Santamouris, and D. Asimakopoulos : Modeling ambient air temperature time series using neural Networks. J Geophysical Research, 103, D16, P.P. 15509-15517, 1998

48

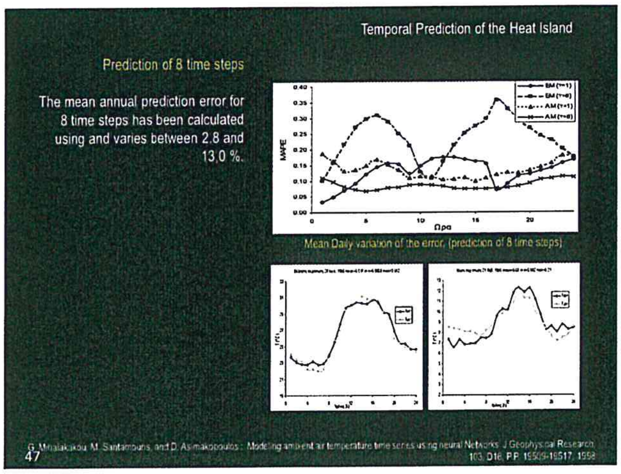
Temporal Prediction of the Heat Island
Prediction of 8 time steps
The mean annual prediction error for 8 time steps has been calculated using and varies between 2.8 and 13,0 %.
MAPE
Ωρα
Mean Daily variation of the error. (prediction of 8 time steps)
G. Mihalakakou, M. Santamouris, and D. Asimakopoulos : Modeling ambient air temperature time series using neural Networks. J. Geophysical Research 103, D16, P.P. 19509-19517, 1998
47

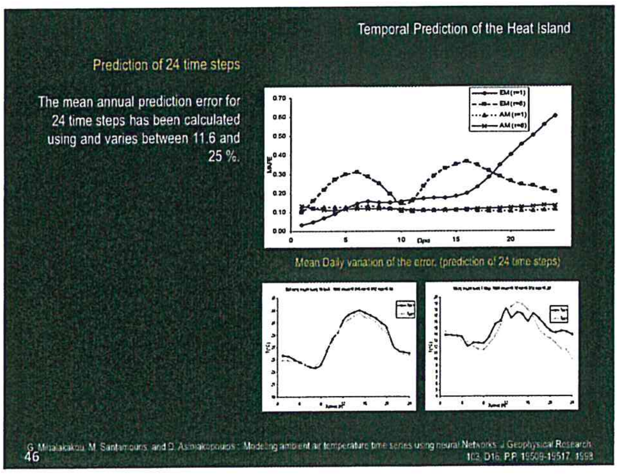
Temporal Prediction of the Heat Island
Prediction of 24 time steps
The mean annual prediction error for 24 time steps has been calculated using and varies between 11.6 and 25 %.
MAPE
Mean Daily variation of the error. (prediction of 24 time steps)
G. Mihalakakou, M. Santamouris, and D. Asimakopoulos : Modeling ambient air temperature time series using neural Networks. J. Geophysical Research 103, D16, P.P. 19509-19517, 1998
46

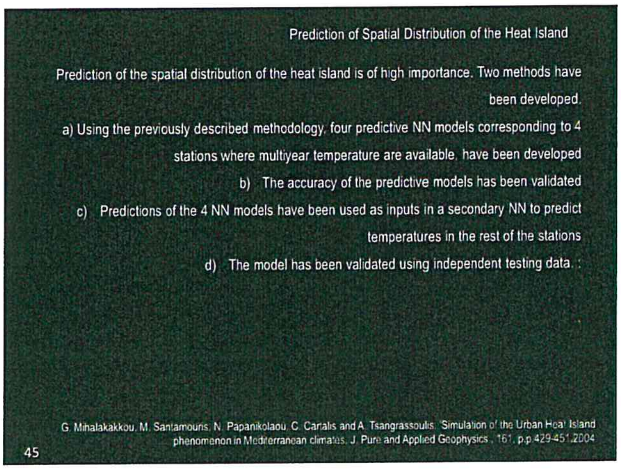
Prediction of Spatial Distribution of the Heat Island
Prediction of the spatial distribution of the heat island is of high importance. Two methods have been developed.
a) Using the previously described methodology, four predictive NN models corresponding to 4 stations where multiyear temperature are available, have been developed
b) The accuracy of the predictive models has been validated
c) Predictions of the 4 NN models have been used as inputs in a secondary NN to predict temperatures in the rest of the stations
d) The model has been validated using independent testing data.
G. Mihalakakou, M. Santamouris, N. Papanikolaou, C. Cartalis and A. Tsangrassoulis. Simulation of the Urban Heat Island phenomenon in Mediterranean climates. J. Pure and Applied Geophysics , 161, p.p.429-451,2004
45

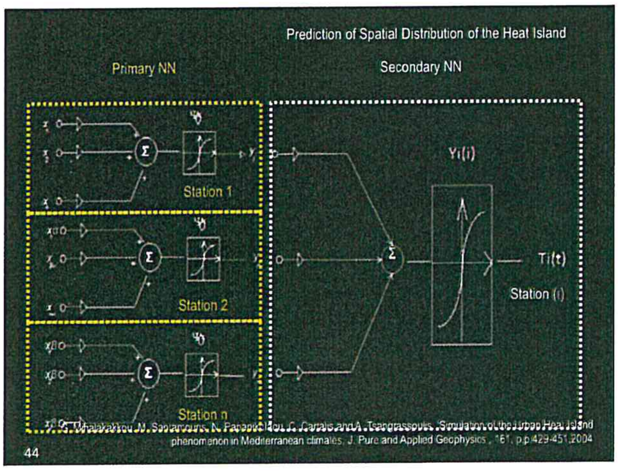
Prediction of Spatial Distribution of the Heat Island
Primary NN
Secondary NN
Station 1
Station 2
Station n
Yi(i)
Ti(t)
Station (i)
G. Mihalakakou, M. Santamouris, N. Papanikolaou, C. Cartalis and A. Tsangrassoulis. Simulation of the Urban Heat Island phenomenon in Mediterranean climates. J. Pure and Applied Geophysics , 161, p.p.429-451,2004
44

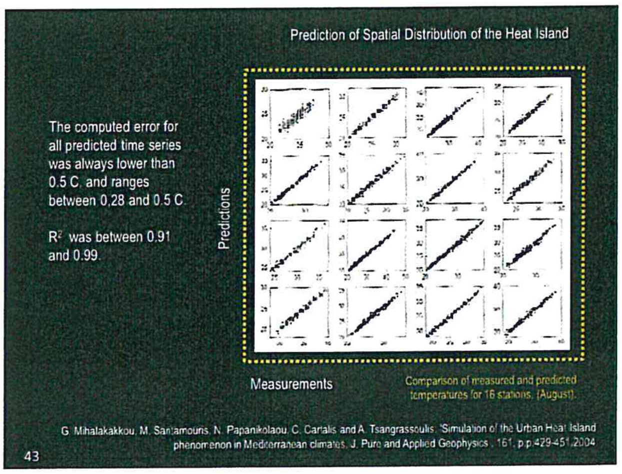
Prediction of Spatial Distribution of the Heat Island
The computed error for all predicted time series was always lower than 0.5 C and ranges between 0.28 and 0.5 C.
R² was between 0.91 and 0.99.
Predictions
Measurements
Comparison of measured and predicted temperatures for 16 stations. (August)
G. Mihalakakou, M. Santamouris, N. Papanikolaou, C. Cartalis and A. Tsangrassoulis. Simulation of the Urban Heat Island phenomenon in Mediterranean climates. J. Pure and Applied Geophysics , 161, p.p.429-451,2004
43

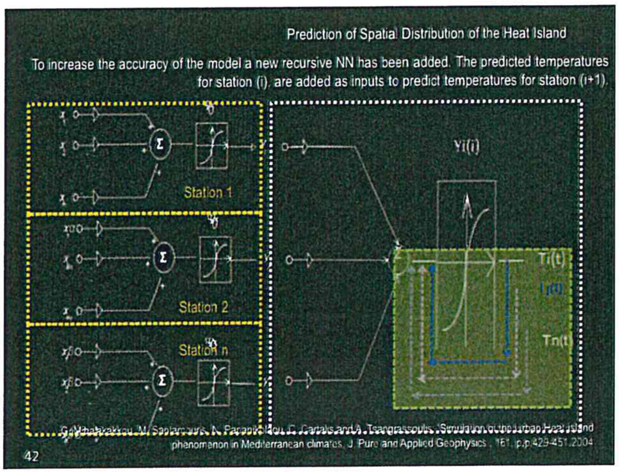
Prediction of Spatial Distribution of the Heat Island
To increase the accuracy of the model a new recursive NN has been added. The predicted temperatures for station (i), are added as inputs to predict temperatures for station (i+1).
Station 1
Station 2
Station n
Yi(i)
Ti(t)
Tn(t)
G. Mihalakakou, M. Santamouris, N. Papanikolaou, C. Cartalis and A. Tsangrassoulis. Simulation of the Urban Heat Island phenomenon in Mediterranean climates. J. Pure and Applied Geophysics , 161, p.p.429-451,2004
42

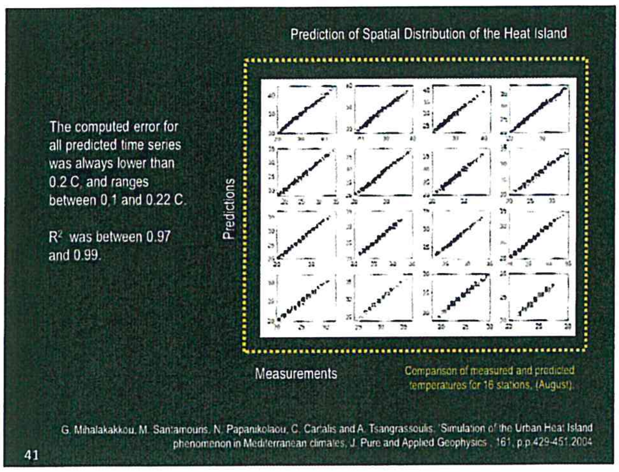
Prediction of Spatial Distribution of the Heat Island
The computed error for all predicted time series was always lower than 0.2 C, and ranges between 0.1 and 0.22 C.
R2 was between 0.97 and 0.99.
Predictions
Measurements
Comparison of measured and predicted temperatures for 16 stations, (August).
G. Mihalakakou, M. Santamouris, N. Papanikolaou, C. Cartalis and A. Tsangrassoulis, Simulation of the Urban Heat Island phenomenon in Mediterranean climates, J. Pure and Applied Geophysics, 161, p.p.429-451,2004
41

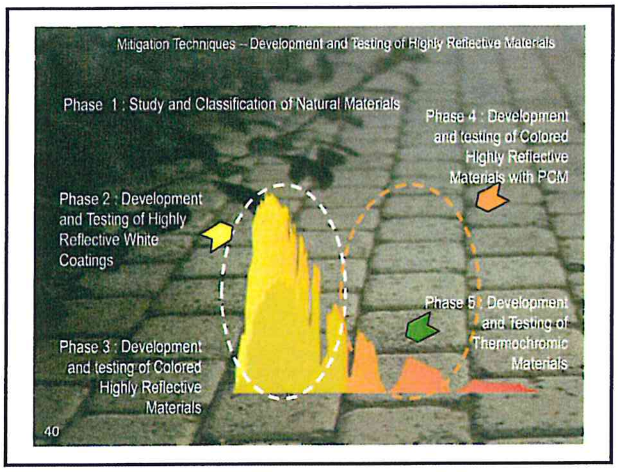
Mitigation Techniques – Development and Testing of Highly Reflective Materials
Phase 1 : Study and Classification of Natural Materials
Phase 2 : Development and Testing of Highly Reflective White Coatings
Phase 3 : Development and testing of Colored Highly Reflective Materials
Phase 4 : Development and testing of Colored Highly Reflective Materials with PCM
Phase 5 : Development and Testing of Thermochromic Materials
40

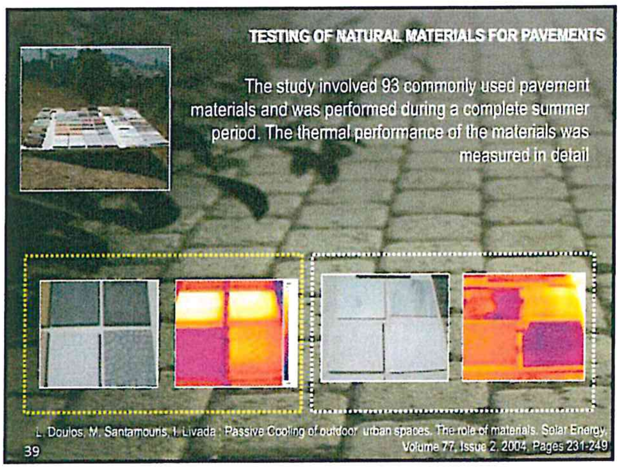
TESTING OF NATURAL MATERIALS FOR PAVEMENTS
The study involved 93 commonly used pavement materials and was performed during a complete summer period. The thermal performance of the materials was measured in detail
L. Doulos, M. Santamouris, I. Livada : Passive Cooling of outdoor urban spaces. The role of materials. Solar Energy, Volume 77, Issue 2, 2004, Pages 231-249
39

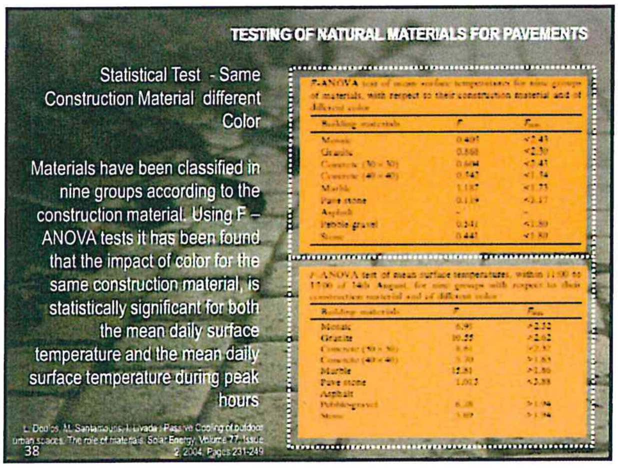
TESTING OF NATURAL MATERIALS FOR PAVEMENTS
Statistical Test - Same Construction Material different Color
Materials have been classified in nine groups according to the construction material. Using F – ANOVA tests it has been found that the impact of color for the same construction material, is statistically significant for both the mean daily surface temperature and the mean daily surface temperature during peak hours
L. Doulos, M. Santamouris, I. Livada : Passive Cooling of outdoor urban spaces. The role of materials. Solar Energy, Volume 77, Issue 2, 2004, Pages 231-249
38

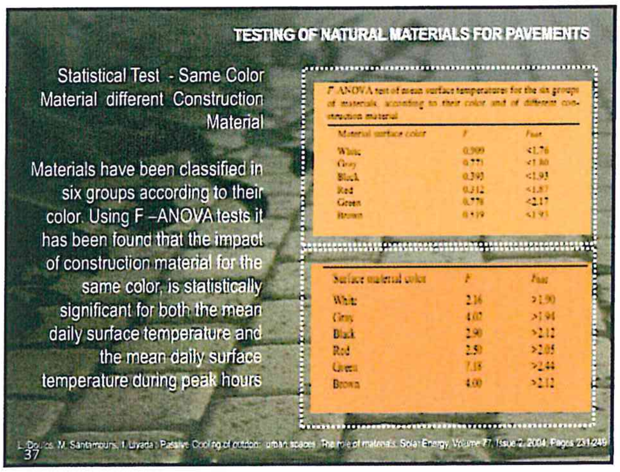
TESTING OF NATURAL MATERIALS FOR PAVEMENTS
Statistical Test - Same Color Material different Construction Material
Materials have been classified in six groups according to their color. Using F –ANOVA tests it has been found that the impact of construction material for the same color, is statistically significant for both the mean daily surface temperature and the mean daily surface temperature during peak hours
L. Doulos, M. Santamouris, I. Livada : Passive Cooling of outdoor urban spaces. The role of materials. Solar Energy, Volume 77, Issue 2, 2004, Pages 231-249
37

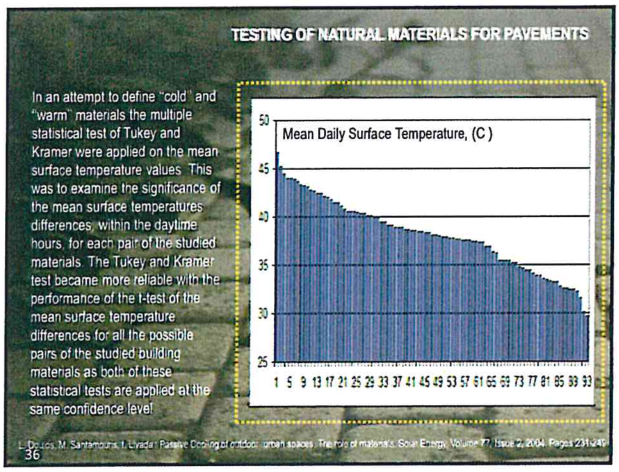
TESTING OF NATURAL MATERIALS FOR PAVEMENTS
In an attempt to define "cold" and "warm" materials the multiple statistical test of Tukey and Kramer were applied on the mean surface temperature values. This was to examine the significance of the mean surface temperatures differences, within the daytime hours, for each pair of the studied materials. The Tukey and Kramer test became more reliable with the performance of the t-test of the mean surface temperature differences for all the possible pairs of the studied building materials as both of these statistical tests are applied at the same confidence level
Mean Daily Surface Temperature, (C)
50
45
40
35
30
25
1 5 9 13 17 21 25 29 33 37 41 45 49 53 57 61 65 69 73 77 81 85 89 93
L. Doulos, M. Santamouris, I. Livada : Passive Cooling of outdoor urban spaces. The role of materials. Solar Energy, Volume 77, Issue 2, 2004, Pages 231-249
36

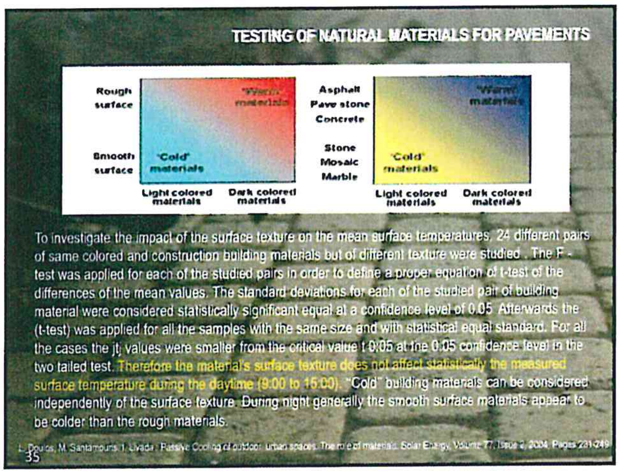

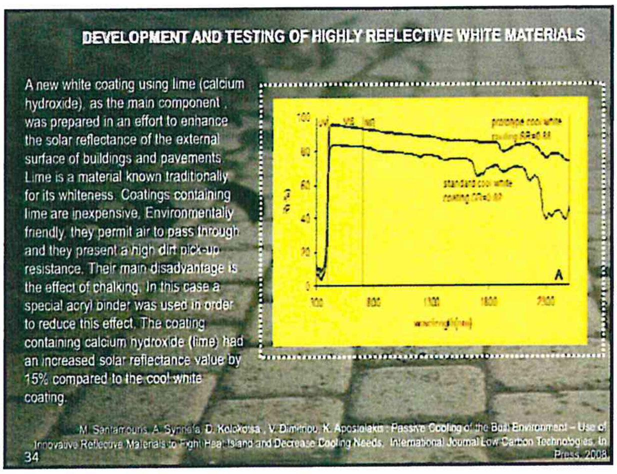

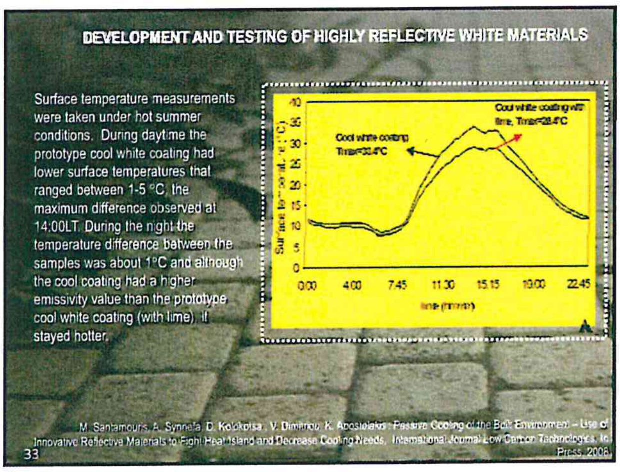

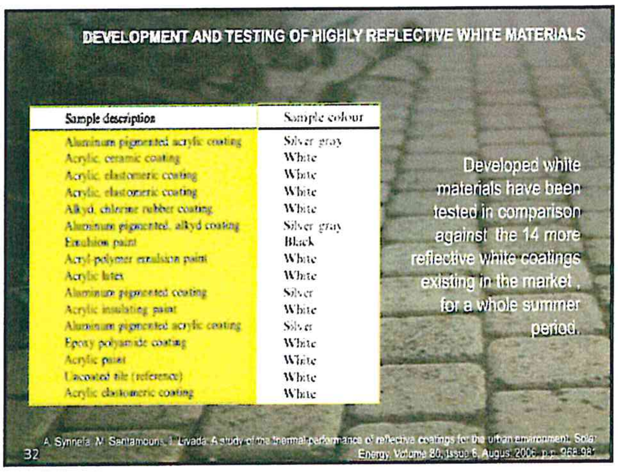

Sample description	Sample colour
Aluminum pigmented acrylic coating	Silver gray
Acrylic, ceramic coating	White
Acrylic, elastomeric coating	White
Acrylic, elastomeric coating	White
Alkyd, chlorine rubber coating	White
Aluminum pigmented, alkyd coating	Silver gray
Emulsion paint	Black
Acryl-polymer emulsion paint	White
Acrylic latex	White
Aluminum pigmented coating	Silver
Acrylic insulating paint	White
Aluminum pigmented acrylic coating	Silver
Epoxy polyamide coating	White
Acrylic paint	White
Uncoated tile (reference)	White
Acrylic elastomeric coating	White

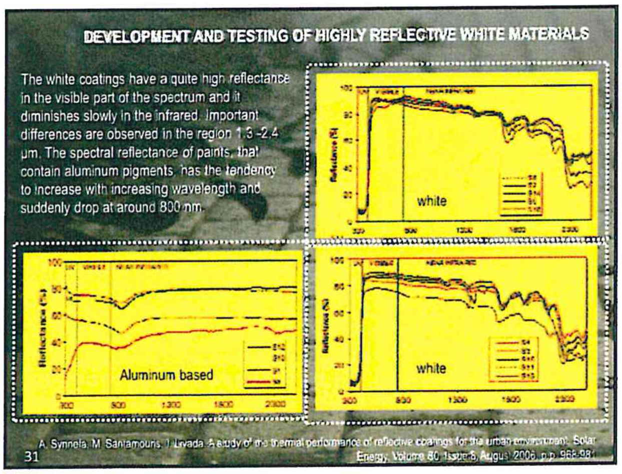

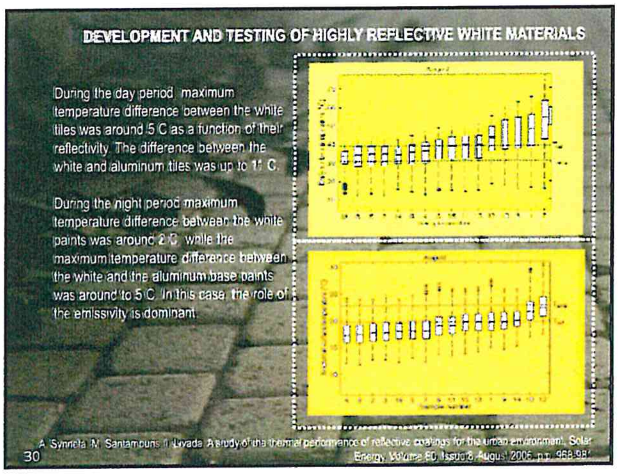

DEVELOPMENT AND TESTING OF HIGHLY REFLECTIVE WHITE MATERIALS

As it was expected white coatings have higher emittance values than aluminum-pigmented coatings. The coating S4 has demonstrated the lower surface temperature during the night and is characterized by the higher emittance value (e = 0.93) among the samples while the sample S12 that maintains the higher surface temperature during the night has the lower emittance value (e = 0.35). It was found that the mean nocturnal surface temperature and the infrared emittance value of the samples are correlated (correlation coefficient = 0.84) and this verifies the fact that during the night, the emissivity is the most important factor affecting the thermal performance of the samples.

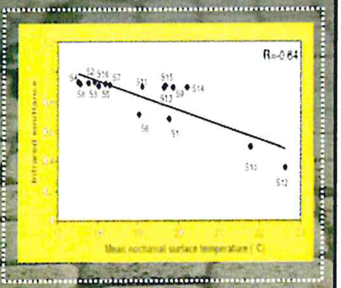

A. Synnefa, M. Santamouris, I. Livada: A study of the thermal performance of reflective coatings for the urban environment. Solar Energy, Volume 80, Issue 8, August 2006, p.p. 968-981

29

DEVELOPMENT AND TESTING OF HIGHLY REFLECTIVE WHITE MATERIALS

A very important factor regarding the thermal performance of coatings is weathering and "dirt pick-up" resistance. Weathering is caused by surface contamination (atmospheric pollution, biological growth) and/or other alterations like UV radiation. white paints absorb in the UV, sudden temperature swings, moisture penetration, etc. The most important change in the thermal behavior was observed for the acrylic elastomeric coating, which was the coolest coating during the daytime period of the first month of the experiment, but became a lot warmer during the second and third month of the experimental period.

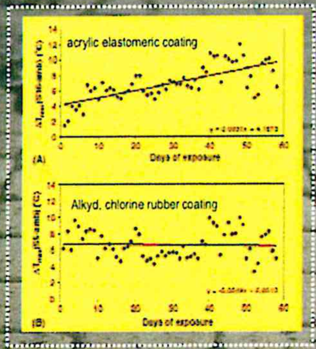

A. Synnefa, M. Santamouris, I. Livada: A study of the thermal performance of reflective coatings for the urban environment. Solar Energy, Volume 80, Issue 8, August 2006, p.p. 968-981

28

DEVELOPMENT AND TESTING OF HIGHLY REFLECTIVE WHITE MATERIALS

ANOVA F test of the means was applied on the surface temperatures of the 16 samples. In an attempt to categorize the coatings and since the ANOVA F test showed that there are significant differences among the mean surface temperatures of the samples, the Tukey and Kramer multiple comparison test of means was performed. The significant level was again chosen to be a = 0.05. On the graph, each samples mean is represented by a circle and an interval around the circle. Two means are significantly different if their intervals are disjoint, and are not significantly different if their intervals overlap.

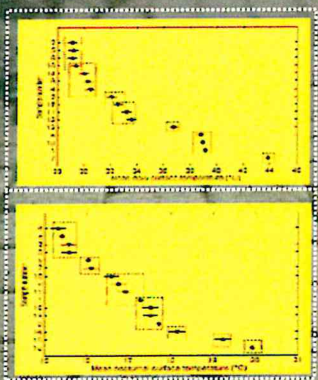

A. Synnefa, M. Santamouris, I. Livada: A study of the thermal performance of reflective coatings for the urban environment. Solar Energy, Volume 80, Issue 8, August 2006, p.p. 968-981

27

DEVELOPMENT AND TESTING OF HIGHLY REFLECTIVE WHITE MATERIALS

During the day, the primary factor affecting the thermal performance of the materials is their color. However, white colored coatings among them present mean surface temperatures that are significantly different. Even coatings that are of the same type, have mean surface temperatures that are significantly different. This is caused by differences in their reflectance. During the night, the surface color does not affect the thermal balance of the samples. The predominant factor regarding the thermal balance of the samples during the night is their emissivity.

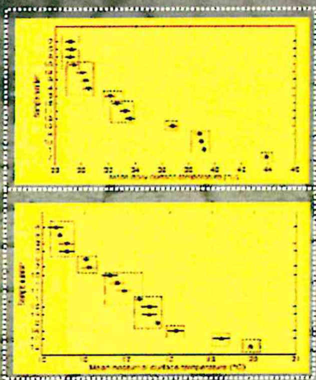

A. Synnefa, M. Santamouris, I. Livada: A study of the thermal performance of reflective coatings for the urban environment. Solar Energy, Volume 80, Issue 8, August 2006, p.p. 968-981

26

DEVELOPMENT AND TESTING OF HIGHLY REFLECTIVE COLORED MATERIALS

The optical properties and the thermal performance of 10 prototype cool colored coatings, prepared at the University of Athens using near-infrared reflective color pigments are tested in comparison to color- matched, conventionally pigmented coatings. The spectral reflectance was measured and the solar reflectance of the samples was calculated. The infrared emittance of the samples was also measured. The surface temperature of the coatings applied to concrete tiles was monitored on a 24 h basis from August to December 2005 in an effort to investigate the ability of the cool colored coatings to maintain lower surface temperatures than conventionally pigmented color-matched coatings under sunlight and during the night during both summer and winter.

A. Synnefa, M. Santamouris and K. Apostolakis: On the development, optical properties and thermal performance of cool colored coatings for the urban environment. Solar Energy 81 (2007) 488-497

25

DEVELOPMENT AND TESTING OF HIGHLY REFLECTIVE COLORED MATERIALS

The spectral characteristics of the cool and conventional materials have been measured and the solar reflectance of each coating is calculated

Color	Solar reflectance (%)		% Increase $SR_{(cool - stand)}$
	Cool	Standard	
Orange	63	35	79
Light blue	42	40	5
Blue	33	18	83
Green	27	20	35
Black (1)	12	6	100
Anthracite	26	7	271
Brown	34	23	48
Chocolate brown	27	9	200
Light brown	36	22	64
Black (2)	27	5	440

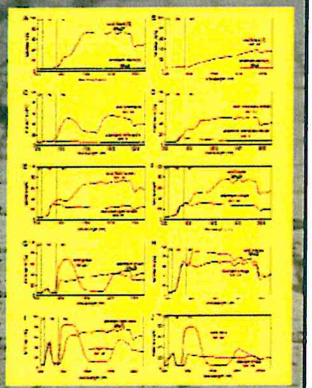

A. Synnefa, M. Santamouris and K. Apostolakis: On the development, optical properties and thermal performance of cool colored coatings for the urban environment. Solar Energy 81 (2007) 488-497

24


DEVELOPMENT AND TESTING OF HIGHLY REFLECTIVE COLORED MATERIALS
During the day, all the cool colored coatings had surface temperatures lower than the colored-matched standard coatings . The best performing cool coatings were black, chocolate brown, blue and anthracite, which maintained differences in mean daily surface temperature from their respective standard color-matched coatings by 5.2, 4.7, 4.7 and 2.8 C, during the month of August. The highest temperature difference was observed between cool and standard black and was equal to 10.2 C, corresponding to a difference in their solar reflectance of 22. The lowest temperature difference was observed between cool and standard green and was equal to 1.6 C (for August) corresponding to a difference in their solar reflectance of 7.
23

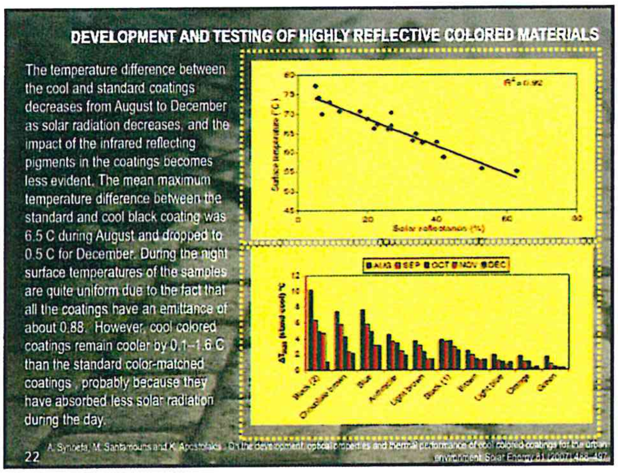
DEVELOPMENT AND TESTING OF HIGHLY REFLECTIVE COLORED MATERIALS
The temperature difference between the cool and standard coatings decreases from August to December as solar radiation decreases, and the impact of the infrared reflecting pigments in the coatings becomes less evident. The mean maximum temperature difference between the standard and cool black coating was 6.5 C during August and dropped to 0.5 C for December. During the night surface temperatures of the samples are quite uniform due to the fact that all the coatings have an emittance of about 0.88. However, cool colored coatings remain cooler by 0.1–1.6 C than the standard color-matched coatings , probably because they have absorbed less solar radiation during the day.
22

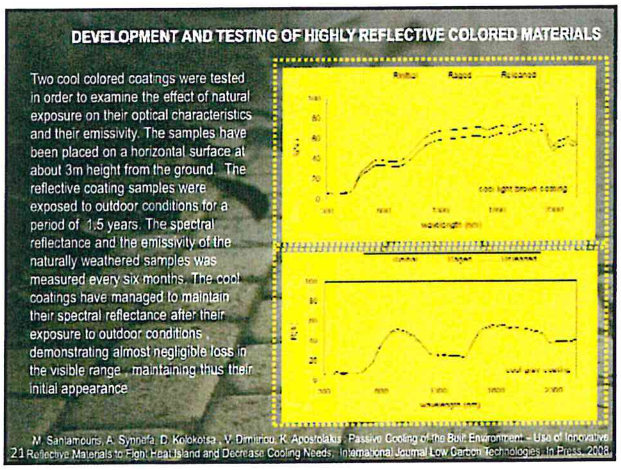
DEVELOPMENT AND TESTING OF HIGHLY REFLECTIVE COLORED MATERIALS
Two cool colored coatings were tested in order to examine the effect of natural exposure on their optical characteristics and their emissivity. The samples have been placed on a horizontal surface at about 3m height from the ground. The reflective coating samples were exposed to outdoor conditions for a period of 1.5 years. The spectral reflectance and the emissivity of the naturally weathered samples was measured every six months. The cool coatings have managed to maintain their spectral reflectance after their exposure to outdoor conditions , demonstrating almost negligible loss in the visible range , maintaining thus their initial appearance
cool light brown coating
cool green coating
21

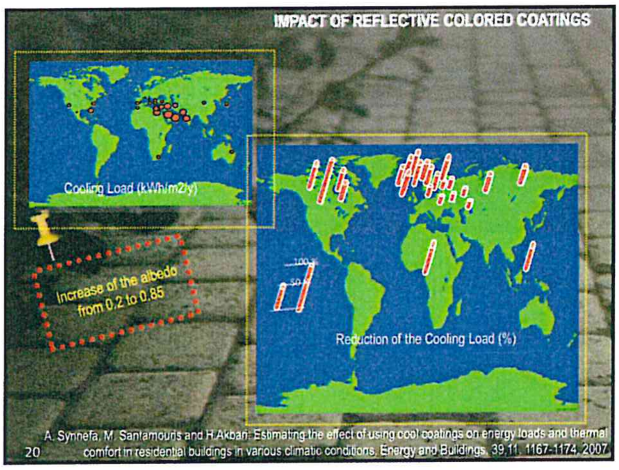
IMPACT OF REFLECTIVE COLORED COATINGS
Cooling Load (kWh/m2/y)
Increase of the albedo from 0.2 to 0.85
Reduction of the Cooling Load (%)
A. Synnefa, M. Santamouris and H.Akbari: Estimating the effect of using cool coatings on energy loads and thermal comfort in residential buildings in various climatic conditions, Energy and Buildings, 39,11, 1167-1174, 2007
20

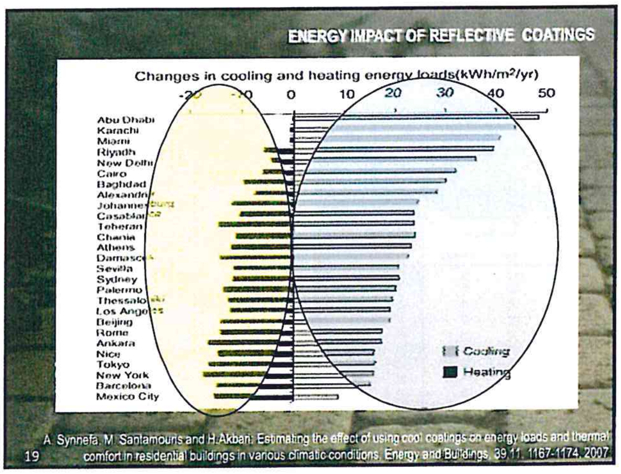
ENERGY IMPACT OF REFLECTIVE COATINGS
Changes in cooling and heating energy loads(kWh/m²/yr)
-20
-10
0
10
20
30
40
50
Abu Dhabi
Karachi
Miami
Riyadh
New Delhi
Cairo
Baghdad
Alexandria
Johannesburg
Casablanca
Teheran
Chania
Athens
Damascus
Sevilla
Sydney
Palermo
Thessaloniki
Los Angeles
Beijing
Rome
Ankara
Nice
Tokyo
New York
Barcelona
Mexico City
Cooling
Heating
A. Synnefa, M. Santamouris and H.Akbari: Estimating the effect of using cool coatings on energy loads and thermal comfort in residential buildings in various climatic conditions, Energy and Buildings, 39,11, 1167-1174, 2007
19

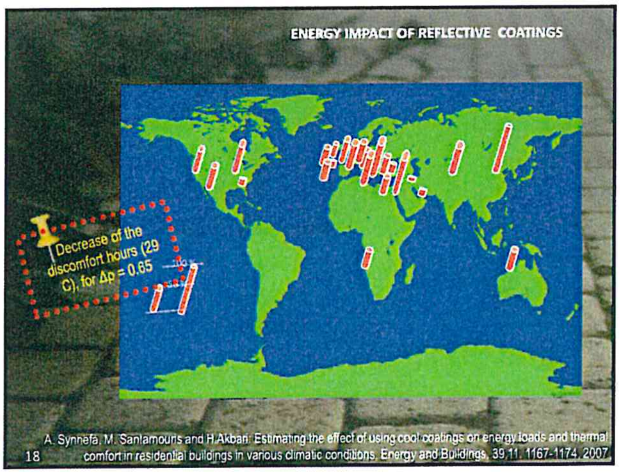
ENERGY IMPACT OF REFLECTIVE COATINGS
Decrease of the discomfort hours (29 C), for Δρ = 0.65
A. Synnefa, M. Santamouris and H.Akbari: Estimating the effect of using cool coatings on energy loads and thermal comfort in residential buildings in various climatic conditions, Energy and Buildings, 39,11, 1167-1174, 2007
18

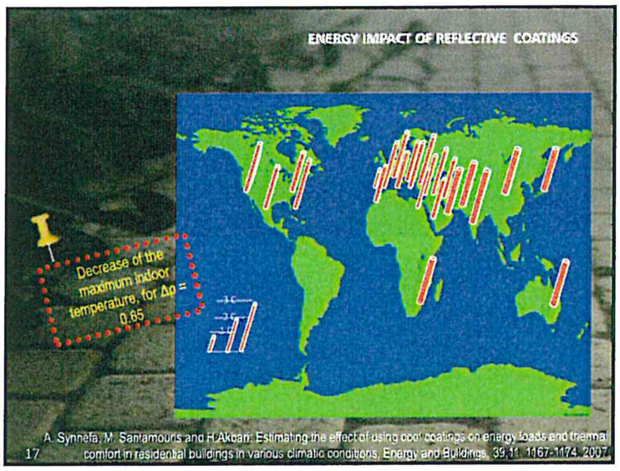

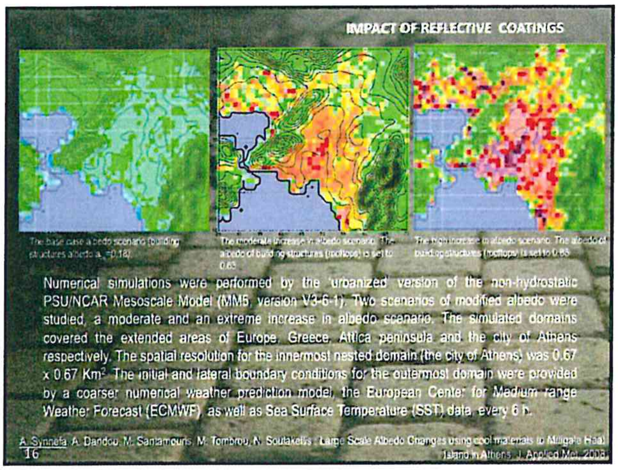

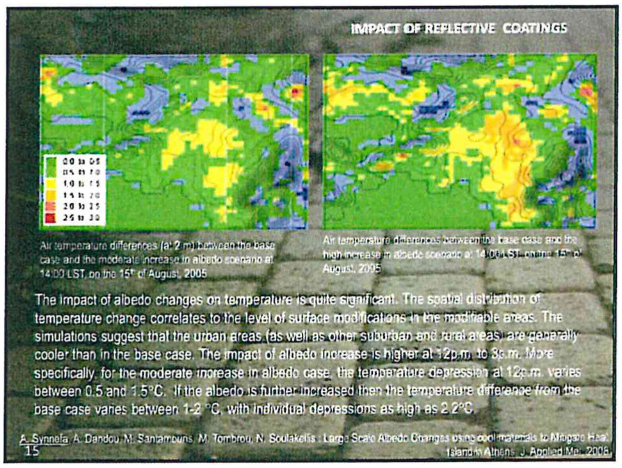

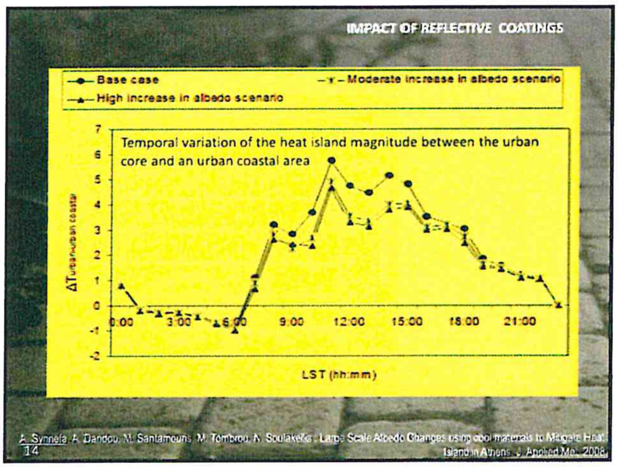

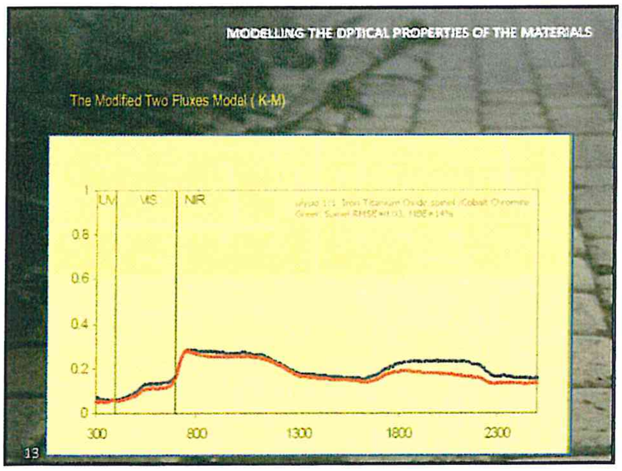

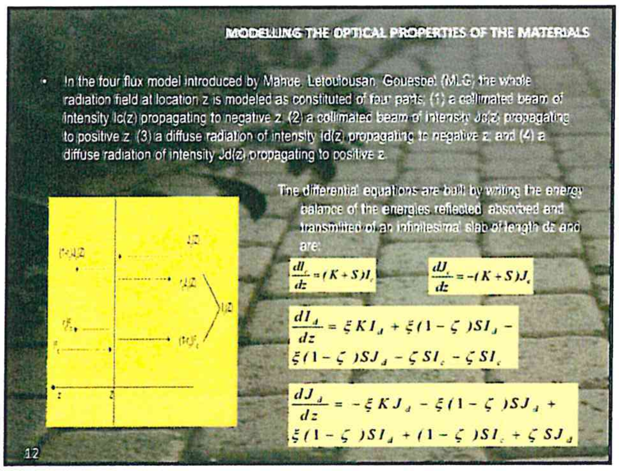

$$\frac{dI_c}{dz} = (K+S)I_c \qquad \frac{dJ_c}{dz} = -(K+S)J_c$$

$$\frac{dI_d}{dz} = \xi K I_d + \xi(1-\zeta)SI_d - \xi(1-\zeta)SJ_d - \zeta SI_c - \zeta SI_c$$

$$\frac{dJ_d}{dz} = -\xi K J_d - \xi(1-\zeta)SJ_d + \xi(1-\zeta)SI_d + (1-\zeta)SI_c + \zeta SJ_d$$

MODELLING THE OPTICAL PROPERTIES OF THE MATERIALS

Preliminary Results are very promising

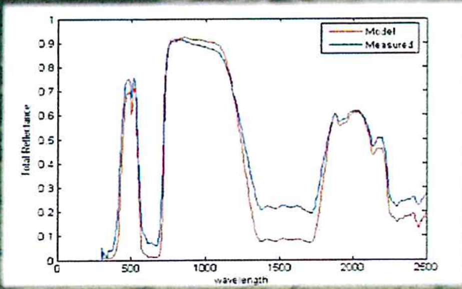

11

USING PCM TO DECREASE SURFACE TEMPERATURE OF REFLECTIVE COLORED MATERIALS

To further decrease the surface temperature of highly reflective colored coating phase change microcaplules containing parafins, (phase change T = 18 C), have been incorporated in the cool coatings. Microcapsules have a diameter of 17-20 μm and are protected externally by a polymeric material. The new materials have been tested quite recently.

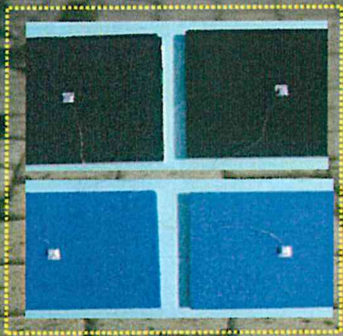

10

USING PCM TO DECREASE SURFACE TEMPERATURE OF REFLECTIVE COLORED MATERIALS

The surface temperature of the black cool material with PCM microcapsules was almost 3,8 C lower than the temperature of the cool black and 13,3 C lower than the common black

Also, the surface temperature of blue cool material with PCM microcapsules was almost 1,8 C lower than the temperature of the cool blue

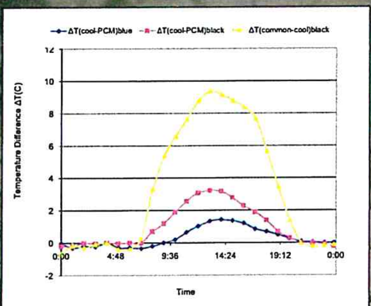

9

DEVELOPEMENT OF THERMOCHROMIC COATINGS

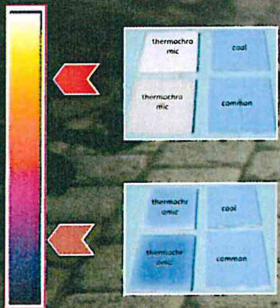

Thermochromic coatings change color as a function of the ambient temperature.
For low outdoor temperatures, winter, the coatings may be dark presenting a high absorptivity.
For higher ambient temperatures, summer, the coating becomes white presenting a high reflectivity.
Thus, when applied on roofs or walls it may present the best performance all year round.

8

DEVELOPEMENT OF THERMOCHROMIC COATINGS

Thermochromism is the reversible colour change of a substance induced by temperature change.

Composition of organic thermochromic dyes

- the color former: usually a cyclic ester which determines the color of the final product in its colored state
- the color developer: usually a weak acid that imparts the reversible color change to the thermochromic material and is responsible for the color intensity of the final product
- the solvent: usually an alcohol or an ester, whose melting point controls the temperature at which the color change occurs

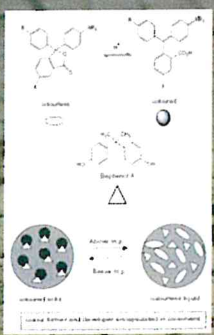

T. Karlessi, M. Santamouris, K. Apostolakis, A. Synnefa, I. Livada : Development and Testing of Thermochromic coatings for Buildings and Urban Structures, Solar Energy, 2008

7

DEVELOPEMENT OF THERMOCHROMIC COATINGS

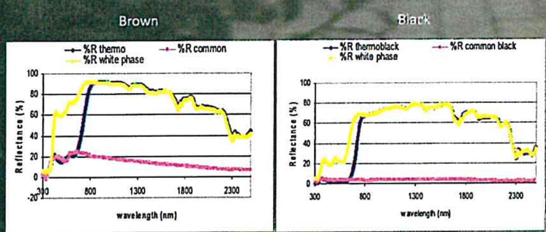

Thermochromic coatings present a high reflectivity both in the visible and infrared spectrum, while present very strong absorption in the near-ultraviolet range of the spectrum.

T. Karlessi, M. Santamouris, K. Apostolakis, A. Synnefa, I. Livada : Development and Testing of Thermochromic coatings for Buildings and Urban Structures, Solar Energy, 2008

6

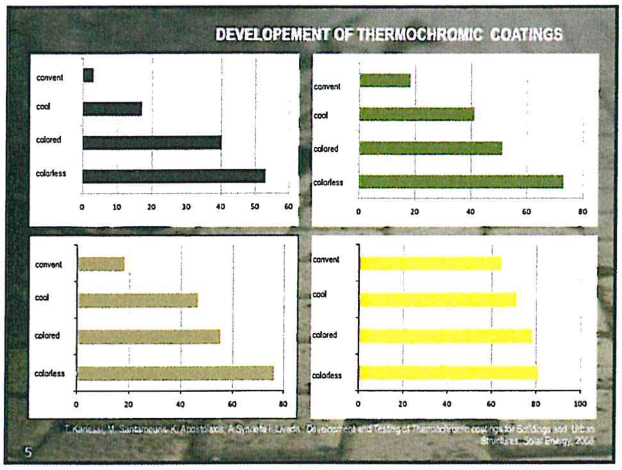
DEVELOPEMENT OF THERMOCHROMIC COATINGS
convent
cool
colored
colorless
T. Karlessi, M. Santamouris, K. Apostolakis, A. Synnefa, I. Livada : Development and Testing of Thermochromic coatings for Buildings and Urban Structures, Solar Energy, 2008
5

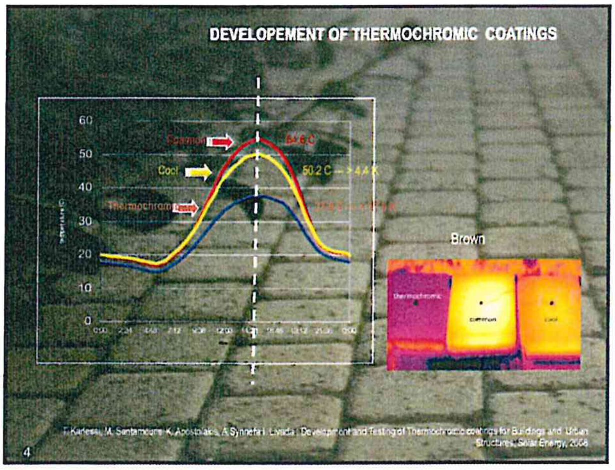
DEVELOPEMENT OF THERMOCHROMIC COATINGS
Cool
Brown
T. Karlessi, M. Santamouris, K. Apostolakis, A. Synnefa, I. Livada : Development and Testing of Thermochromic coatings for Buildings and Urban Structures, Solar Energy, 2008
4

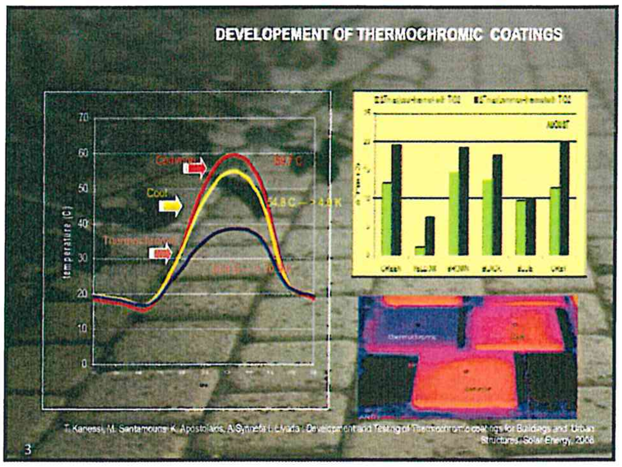
DEVELOPEMENT OF THERMOCHROMIC COATINGS
Cool
temperature (C)
T. Karlessi, M. Santamouris, K. Apostolakis, A. Synnefa, I. Livada : Development and Testing of Thermochromic coatings for Buildings and Urban Structures, Solar Energy, 2008
3

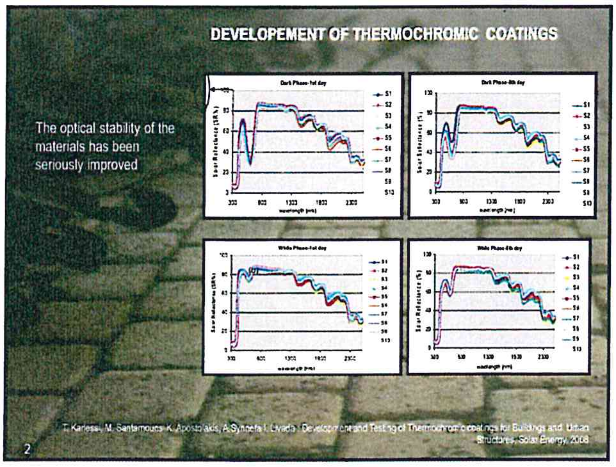
DEVELOPEMENT OF THERMOCHROMIC COATINGS
The optical stability of the materials has been seriously improved
T. Karlessi, M. Santamouris, K. Apostolakis, A. Synnefa, I. Livada : Development and Testing of Thermochromic coatings for Buildings and Urban Structures, Solar Energy, 2008
2


DEVELOPEMENT OF THE EUROPEAN COUNCIL FOR COOL ROOFS
The European Union has financed through the IEE Program the research project 'COOL ROOFS' that aims to promote cool materials and cool roofs in Europe for buildings and open spaces.
The program has to investigate the potential of cool materials, promote their use through real applications of excellent, organise the market and set the rules for the promotion and use of cool materials
The program will start in September 2008 and will end at 2010.
The assistance of LBNL and in Particular of Dr H. Akbari is highly acknowledged
1

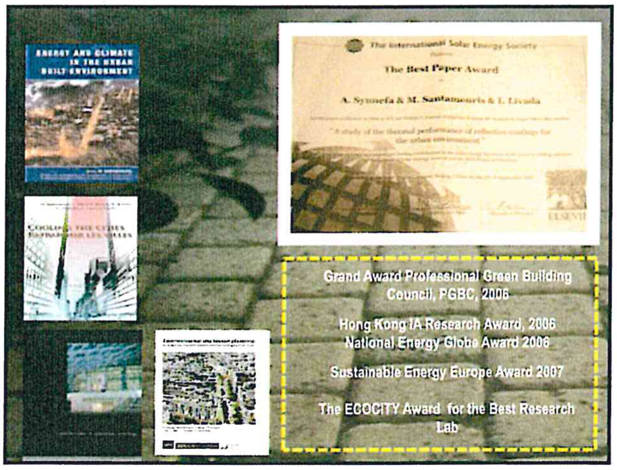
ENERGY AND CLIMATE IN THE URBAN BUILT ENVIRONMENT
The Best Paper Award
A. Synnefa & M. Santamouris & I. Livada
Grand Award Professional Green Building Council, PGBC, 2006
Hong Kong IA Research Award, 2006
National Energy Globe Award 2006
Sustainable Energy Europe Award 2007
The ECOCITY Award for the Best Research Lab

Available online at www.sciencedirect.com
ScienceDirect
Solar Energy xxx (2008) xxx–xxx
ELSEVIER
Solar Energy
www.elsevier.com/locate/solener

Development and testing of thermochromic coatings for buildings and urban structures

T. Karlessi [a,*], M. Santamouris [a], K. Apostolakis [b], A. Synnefa [a], I. Livada [a]

[a] *Group Building Environmental Studies, National and Kapodistrian University of Athens, Section of Applied Physics, Physics Department, Build. Physics 5, 15784 Athens, Greece*
[b] *Colors Chemical Industry, Greece*

Received 14 December 2007; received in revised form 13 August 2008; accepted 4 October 2008

Communicated by: Associate Editor Darren Bagnall

Abstract

The present study reports the development and comparative testing of thermochromic coating to be used in buildings and urban structures. Experimental results from an extensive comparative analysis of the thermal and physical behaviour of thermochromic, highly reflective (cool), and common coatings are reported and analyzed. The surface temperature was monitored on 24 h basis from August to mid-September 2007. It was revealing that the temperature of thermochromic coatings was lower than cool and common coatings. Measurements of spectral reflectance indicated that the thermochromic coatings at the colored phase (below the transition temperature of 30 °C) are energy-absorbing while at the colorless phase (above the transition temperature of 30 °C) are energy-reflecting. The data obtained was used for the calculation of solar reflectance. The results showed that the solar reflectance of the thermochromic samples was significally higher compared to the cool and common ones. A 10-day period test was also performed showing the impact of solar radiation on thermochromism.

The comparative results demonstrate that the use of thermochromic coatings can both contribute to energy savings in buildings, providing a thermally comfortable indoor environment, while can contribute highly to improve the urban microclimate.

Keywords: Thermochromic coatings; Organic leuco dye mixture; Urban heat island; Cool paints; Urban microclimate

1. Introduction

Heat island is the more documented climatic change phenomenon (Santamouris, 2001). Important research has been carried out to document its strength and its influence on the urban climate (Santamouris, 2007; Akbari et al., 1999). Heat island intensity in hot climates may rise up to 10 °C (Livada et al., 2002; Mihalakakou et al., 2002, 2004; Santamouris et al., 1999), resulting in increased discomfort, higher pollution levels while it has a serious impact on the cooling energy consumption of buildings (Hassid et al., 2000). Increased urban temperatures, exacerbate the peak electricity demand for cooling and decrease the efficiency of air conditioners (Santamouris et al., 2001), while it reduces considerably the cooling potential of natural and night ventilation techniques (Geros et al., 2005) and increases the urban ecological footprint (Santamouris et al., 2007).

Various mitigation techniques to fight heat island have been proposed (Santamouris et al., 2004). Selection of appropriate materials to be used in the urban fabric can contribute to the improvement of the urban microclimate, the decrease of the energy loads of the buildings and the reduction of air pollution.

The main properties of a material that control its surface temperature are the solar reflectance and the infrared

* Corresponding author. Tel.: +302107274092; fax: +302107295282.
E-mail addresses: karlessi@ath.forthnet.gr , karlessith@phys.uoa.gr (T. Karlessi).

0038-092X/$ - see front matter © 2008 Published by Elsevier Ltd.
doi:10.1016/j.solener.2008.10.005

emittance (Akbari and Bretz, 1997). Increased values of reflectance and/or emittance result in lower surface temperatures. Regarding the building's performance, lower surface temperatures decrease the heat penetrating into the building and, therefore, decrease the cooling loads in case of air-conditioned buildings, or create more comfortable thermal conditions in case of non-air-conditioned buildings. Regarding the urban environment, it contributes to the decrease of the ambient air temperature, mitigating the heat island effect (Synnefa et al., 2007a; Akbari et al., 1992; Berdahl and Bretz, 1997; Bretz et al., 1997). The performance of materials with high solar reflectance and infrared emittance values, known as cool materials, has been extensively studied (Berdahl and Bretz, 1997; Bretz et al., 1997; Rosenfeld et al.,1996; Synnefa et al., 2006, 2007b,c; Bretz and Akbari, 1997; Prado and Ferreira, 2005). An increase in roof albedo of 0.4 resulted in peak cooling demand savings of 20–40% in residences and 5–10% in offices at the Los Angeles basin, as proved by building energy simulations (Akbari et al., 1999). In the area of Athens, Greece, the use of a mesoscale model has demonstrated that an increase in building structures albedo of 0.65 can decrease the air temperature by 2.2 °C (Synnefa et al., 2007a). Light colored coatings, when applied on external building surfaces can decrease the cooling load during summer period. During winter period though, in order to reduce energy consumption for heating, the increase of solar gains is required. As shown in Synnefa et al. (2007b) the use of highly reflective coatings on the roof of buildings may cause a heating penalty in zones where heating is important. Thus, there is a need for the development of a technology that can change the optical properties of a material according to the outdoor temperature and solar radiation levels.

Color-changing compounds have become increasingly important in recent years in the study and the production of thermochromic coatings, that is coatings which respond thermally to their environment, changing reversibly their color from darker to lighter tones as temperature rises (Azari and Bierman, 2005; Watts et al., 2006; Ma et al., 2001, 2002). The transition is achieved by a thermally reversible transformation of the molecular structure of the pigments that produces a spectral change of visible color (McNaught and Wilkinson, 1997; Aitken et al., 1996; White and LeBlanc, 1999). A major approach elucidating this alteration is based on organic leuco dye mixtures whose three main components are: the color former, usually a cyclic ester which determines the color of the final product in its colored state, the color developer, usually a weak acid that imparts the reversible color change to the thermochromic material and is responsible for the color intensity of the final product and the solvent, usually an alcohol or an ester, whose melting point controls the transition temperature at which the color change occurs. In order to maintain the thermochromic properties, the mixture is encapsulated in microcapsules of less than 15 μm. Microencapsulation serves as a barrier between the thermochromic system and the chemicals around it, such as the paint base, protecting the system from weather conditions, oxidation etc. (Aitken et al., 1996; White and LeBlanc, 1999; Bamfield, 2001; Yoshikawa et al., 1986; Novinson, 1996; Fujita and Senga, 2002; Shibahashi et al., 1984; MacLaren and White, 2003a,b; White et al., 2000).

Thermochromic pigments have been developed as three-component organic mixtures and they were incorporated into common white coating (Ma et al., 2001, 2002). Measurements of the solar reflectance spectra of thermochromic building coatings have been carried out and the results showed that the absorption of solar energy is higher below the transition temperature of 20 °C and lower above 20 °C (Ma et al., 2001). After an hour of exposure to solar radiation and for ambient temperatures below 20 °C the thermochromic coating could absorb almost the same amount of solar energy as an ordinary colored coating, but when the temperature was above 20 °C it could reflect more solar energy, presenting 4 °C lower temperature than the ordinary colored coating (Ma et al., 2002).

The results from the use of thermochromic black pigments on white textile membranes for building coverings demonstrated that during the summer period when the incident solar radiation increased by approximately 50%, the thermal flux that passed through the membrane slightly decreased by 7.7% when the color changed from black to white (Neves, 2001).Organic polymeric materials such as coatings, exposed to outdoor conditions, degrade over time due to temperature variations, atmospheric pollution and solar radiation triggered processes (Pospisil and Nespurec, 2000; Berdahl et al., 2008). The absorption of UV energy can cause the breaking and/or crosslinking of the polymer chains, leading to altered chemical and mechanical properties (Berdahl et al., 2008). Solar reflectance and infrared emittance are properties of the coating that may change over time as a result of aging. Results from a three-month period of outdoor exposure of building coatings indicate that the coatings which have the higher initial solar reflectance are the ones that demonstrate the higher decrease in solar reflectance (Synnefa et al., 2007c). A thermochromic organic coating which did not contain an agent for improving light fastness presented color density attenuation of 60%, after 50 h of exposure to a carbon arc light (Fujita et al., 1997).

The cost of thermochromic materials is currently high, however widespread uptake by the construction industry would lead to a scale-up in production and significant cost reduction. The advantages that can be derived from their color-changing properties concerning energy efficiency in buildings, indoor air environment and urban microclimate encourages further investigation.

The present study examines the thermal and optical characteristics of 11 developed thermochromic coatings to be used in buildings and urban structures. Coatings have been produced using available organic thermochromic pigments incorporated into an appropriate binder system and other stabilizing components to develop a thermochromic paint. The coatings produced have been experimentally compared against common and highly reflective coatings of the same color.

Outdoor measurements of surface temperature were carried out in an hourly basis from August to mid-September 2007 using temperature sensors on concrete tiles coated with thermochromic, cool and common paint. Furthermore, the spectral reflectance and the infrared emittance were measured and the solar reflectance of the samples was calculated. Aging of the thermochromic coatings is also studied and discussed.

2. Development of thermochromic building coatings

Organic water based thermochromic pigments of powder and slurry form were used (Color Change Corporation, 2007; Cornelius Group PLC, 2007) to develop the thermochromic coatings. All pigments were colored in their cold state and translucent in their warm state having a transition temperature of 30 °C. Pigments were microencapsulated with an average particle size of 5 μm. The content in solid thermochromic compound of the thermochromic pigment in its slurry form is 50%. An appropriate binder system that should not itself absorb infrared radiation was produced for the development of the thermochromic coatings. In order to examine the behaviour of thermochromic pigments without the interference of any other type of pigments and simultaneously avoid transparency of the coating at the warm state, two groups of thermochromic coatings were prepared: the first one comprised of the thermochromic pigments and the binder, and the second of the thermochromic pigments, the binder and titanium dioxide (TiO_2). For each of the six colors, two coatings were prepared, one with the addition of TiO_2, and the other without TiO_2. Coatings without TiO_2 are translucent, the presence of TiO_2 gives hiding power to the coating which means that it gives the ability to obscure the surface over which it has been applied (Cremer, 1981). Especially for brown, only the coating with TiO_2 was examined because the color of the thermochromic coating without TiO_2 did not match with any cool brown coating, so 11 thermochromic coatings in total were developed.

2.1. Grouping of the coatings

Cool coatings, that means coatings that are characterized by high solar reflectance and infrared emittance values (Synnefa et al., 2007c), were produced with the same binder system as thermochromic coatings.

The quantity of TiO_2 that was added was the same for all coatings. The groups of color-matched thermochromic, cool and conventionally pigmented (common) coatings are shown in Fig. 1. Thermochromic coatings are presented at their colored phase for temperatures lower than 30 °C.

The coatings were applied on white concrete tiles placed on an unshaded horizontal platform insulated from below. The size of the tiles was 33 cm × 33 cm.

Fig. 2 depicts the color-changing phase of the thermochromic coatings. Surface temperature of the tiles is lower than the transition temperature of 30 °C thus thermochromic coatings are fully colored (Fig. 2a), while their color starts to fade and they are becoming colorless as their temperature gets higher than 30 °C (Fig. 2b).

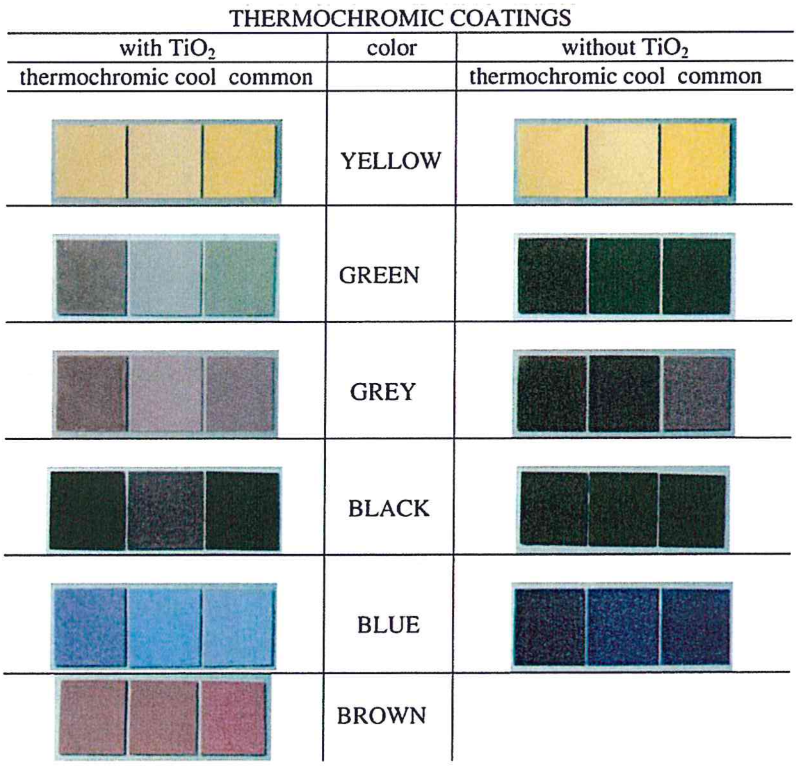

Fig. 1. The developed and tested thermochromic, cool and common color-matched coatings.

Please cite this article in press as: Karlessi, T. et al., Development and testing of thermochromic coatings for buildings ..., Sol. Energy (2008), doi:10.1016/j.solener.2008.10.005

In Fig. 3a and b, on the left, color-changing phase of thermochromic green coating with TiO_2 is shown. On the right, the tile with the cool coating of the same color is shown as well. Fig. 3a depicts the color of the tiles 15 min after exposure to outdoor conditions at a warm day with clear sky and ambient temperature of 35 °C. When the surface temperature is increasing above 30 °C, the thermochromic coating has started changing color from green to white due to its temperature increase. The coating has turned almost white 20 min after outdoors exposure, as it is shown in Fig. 3b, when its surface temperature has become 37 °C. Thermochromic blue coatings are presented at the left side of Fig. 3c–e, with TiO_2 on top, without TiO_2 on bottom, becoming white and transparent, respectively, as surface temperature rises above 30 °C. Fig. 3c depicts their color 7 min after outdoor exposure where the color has started to change. The color change is becoming more obvious in Fig. 3d 10 min after outdoor exposure. The thermochromic coatings are completely decolorized 20 min later as their surface temperature has become 42 °C (Fig. 3e).

3. Experimental procedure

3.1. Instrumentation, measurements and climatic data

For the investigation of the thermal and optical performance of the coatings, the following equipment was used:

(i) Surface mounted type K thermocouples were placed at the centre of each tile and temperature was measured every 10 min on a 24 h basis using a data logging system based on an Analog to Digital converter (ADAM408).
(ii) An infrared camera (AGEMA Thermovision 570 7.5–13 μm wavelength), was used for observing the temperature difference between the samples.
(iii) UV/vis/NIR spectrophotometer (Varian Carry 5000), was used for measuring the spectral reflectance of the samples. The spectrophotometer is fitted with a 150 mm diameter, integrating sphere (Labsphere DRA 2500) which collects both specular and diffuse radiation. The reference standard reflectance material used for the measurement was a PTFE plate (Labsphere).
(iv) An emissometer model AE of the Devices and Services, was used for the measurement of the infrared emittance of the samples. The total thermal emittance is determined by the instrument in comparison with standard high and low emittance materials.

Measurements were performed in Athens in August and September 2007 while supporting meteorological data was recorded by the nearby National Observatory of Athens, including ambient temperature, relative humidity, wind speed, global and diffuse solar radiation on a horizontal surface (Table 1). During the experimental period, high temperatures, clear skies and low wind speeds were the

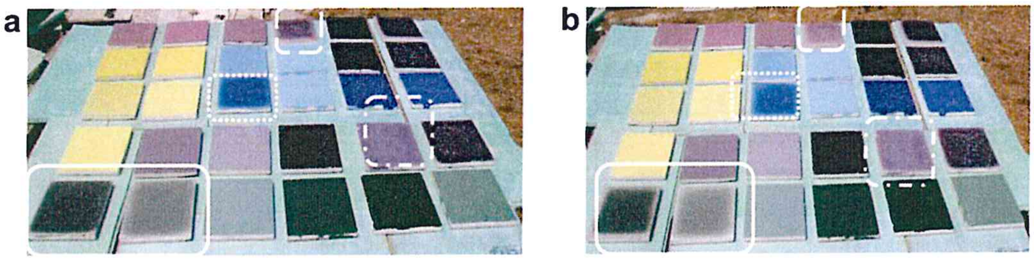

Fig. 2. Color-changing phase of the thermochromic coatings. Colored state below 30 °C (a), start becoming colorless above 30 °C (b).

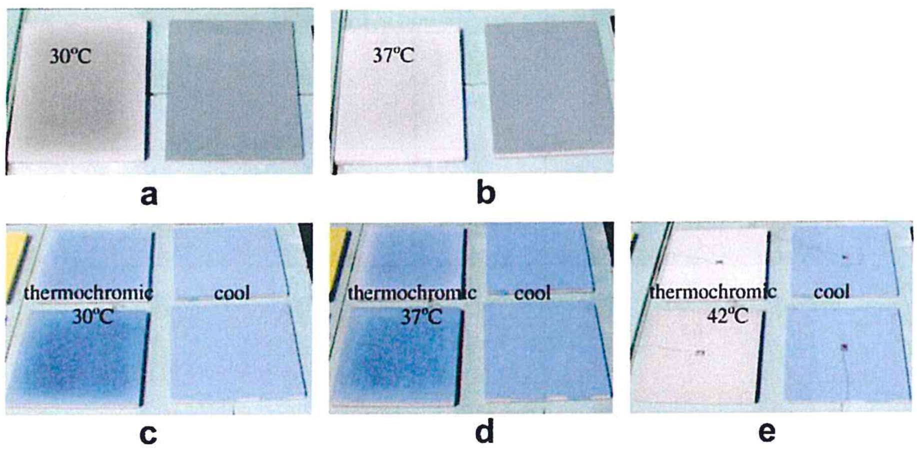

Fig. 3. Transition phase of thermochromic green (a), (b), and blue (c), (d), (e) coatings. Thermochromic coatings are on the left side, becoming white as temperature rises above 30 °C. On the right side color-matched cool coating are presented.

Please cite this article in press as: Karlessi, T. et al., Development and testing of thermochromic coatings for buildings ..., Sol. Energy (2008), doi:10.1016/j.solener.2008.10.005

Table 1
Meteorological parameters during the experimental period.

Months	T_{amb} (°C)			RH%	Wind speed (m/s)	Monthly average daily diffuse solar radiation (W/m²)	Monthly average daily global solar radiation (W/m²)
	Mean	Maximum	Minimum				
August	29.2	35.1	24.7	44	3.6	1410	6664
September	23.9	29.9	19.9	54	3.2	1185	5357

dominating meteorological conditions. In Fig. 4 the monthly average hourly diffuse and global solar radiation (W/m²) on a horizontal surface for the experimental period is presented.

4. Comparative analysis of the thermal performance of thermochromic coatings

Infrared imaging was used to reveal temperature differences between thermochromic, cool and common coatings. Visible and infrared images were taken at the time of maximum temperature of a representative summer day.

In Fig. 5, blue samples with TiO_2 and black samples without TiO_2 are depicted at the visible and the infrared part of the solar radiation. Thermal imaging presents the temperature differences between thermochromic, cool and common coatings. High ambient temperatures result in high surface temperatures of the samples. The surface temperature of the blue thermochromic coating (Fig. 5a) is 35 °C, so its color has become white. Considering the infrared temperature scale (Fig. 5b), thermochromic blue coating presents lower temperatures than cool and common. This accounts for thermochromic black coating as well (Fig. 5c and d). Comparing thermochromic blue coating with TiO_2 and thermochromic black coating without TiO_2 at their colorless state, blue coating has become white, due to the presence of TiO_2, while black coating has become translucent, presenting higher temperature than the blue coating.

In order to observe the temperatures that the thermochromic coatings demonstrate and to compare them with the temperatures of the corresponding cool and common coatings, the mean daily, mean maximum daily (6:00–20:00) and nocturnal (0:00–6:00, 20:00–24:00) surfaces temperatures of the samples were calculated from the measured data. The average value of the instantaneous (every 10 min) measured temperatures from 6:00 to 20:00 for each day and for each sample was calculated and used for obtaining the mean daily surface temperature for each month. The same accounts for the mean nocturnal surface temperature from 0:00 to 6:00 and from 20:00 to 24:00. Mean maximum daily surface temperatures for each month are obtained by the average of the maximum daily temperature values.

The results for each sample are demonstrated in Table 2, for August and September. For each color and type of coating during the experimental period the samples with TiO_2 (lighter tones) demonstrate lower temperatures than the samples without TiO_2 (darker tones). Light colored common coatings correspond to thermochromic and cool coatings with TiO_2, while dark colored common coatings correspond to thermochromic and cool coatings without TiO_2.

Mean daily surface temperatures range from 31 to 38.4 °C for the thermochromic coatings, from 34.4 to 45.2 °C for cool coatings and from 36.4 to 48.5 °C for common coatings in August. In September, mean daily surface temperatures vary from 26.1 to 31.6 °C for thermochromic coatings, from 28.1 to 39.2 °C for cool coatings and from 29.8 to 42.3 °C for common coatings.

Comparing the group of thermochromic, cool and common coatings with TiO_2 the following are observed:

Mean daily surface temperatures of thermochromic coatings are lower than cool and common coatings. During August, temperature difference range from 2.2 °C for thermochromic and cool yellow to 9.2 °C for thermochromic and cool brown and from 4.2 °C for thermochromic and

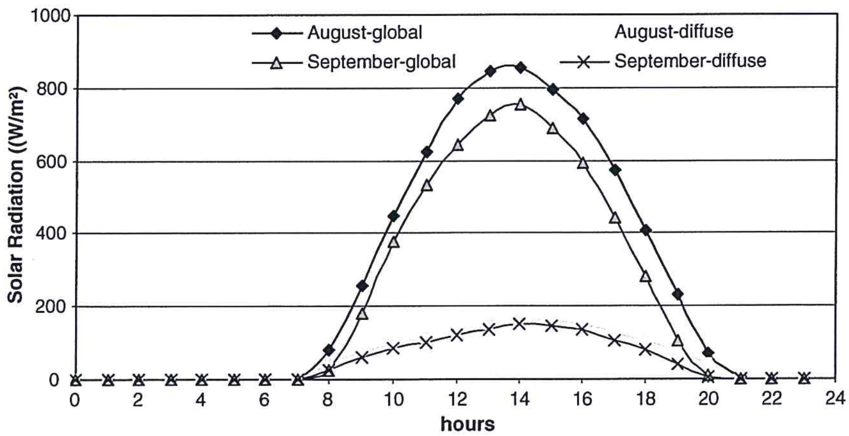

Fig. 4. Monthly average hourly diffuse and global solar radiation (W/m²) on a horizontal surface for the experimental period.

Please cite this article in press as: Karlessi, T. et al., Development and testing of thermochromic coatings for buildings ..., Sol. Energy (2008), doi:10.1016/j.solener.2008.10.005

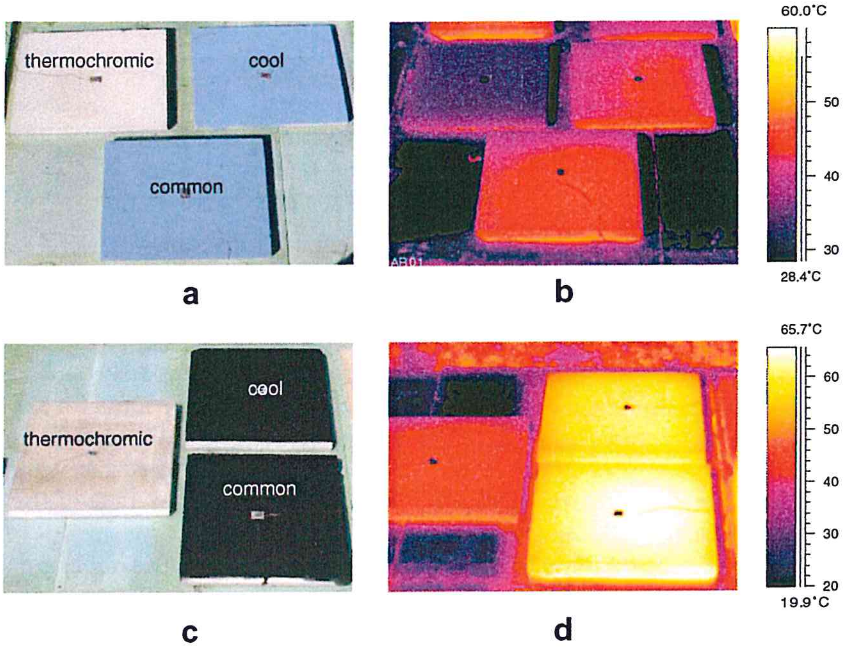

Fig. 5. Temperature differences of thermochromic, cool and common coatings: visible (a), (c) and infrared (b), (d) images of blue coatings with TiO_2 and black coatings without TiO_2, respectively.

common yellow to 11.4 °C for thermochromic and common green. Temperature differences are a little higher in September, ranging from 3.2 °C between thermochromic and cool yellow to 10.4 °C for thermochromic and cool brown and from 4.9 °C for thermochromic and common yellow to 12.1 °C for thermochromic and common brown.

In August, thermochromic coatings demonstrate 10–15 °C lower mean max daily temperatures than cool coatings, except from yellow ($\Delta T_{max(cool-thermo)} = 1.5$ °C) and 18–20 °C lower than common coatings, except from yellow ($\Delta T_{max(common-thermo)} = 6.8$ °C) and blue ($\Delta T_{max(common-thermo)} = 10.1$ °C) (Fig. 6). In September, differences increase ($\Delta T_{max(cool-thermo)} = 11$–$17$ °C) between thermochromic and cool coatings, except from yellow ($\Delta T_{max(cool-thermo)} = 6.6$ °C) while differences between thermochro mic and common coatings are of 19–22 °C, apart from yellow ($\Delta T_{max(common-thermo)} = 7.8$ °C) and blue ($\Delta T_{max(common-thermo)} = 11.7$ °C).

Comparing the group of thermochromic, cool and common coatings without TiO_2 the following are remarked:

Thermochromic coatings demonstrate lower mean daily temperatures than cool and common coatings. In August temperature difference range from 2.8 °C for thermochromic and cool yellow to 8.9 °C for thermochromic and cool grey and from 3.9 °C for thermochromic and common yellow to 12.5 °C for thermochromic and common green. Until mid-September, maximum temperature difference of 9.3 °C between thermochromic and cool coatings is noticed for the green color, while yellow color exhibits the minimum temperature difference of 2.4 °C. Thermochromic coatings, compared to common coatings present temperature differences which range from 3.6 °C for the yellow coating to 13.7 °C for the green coating.

In August, mean maximum daily surface temperatures are 10–16 °C lower for thermochromic coatings compared to cool coatings except from yellow coating which demonstrates 2.9 °C lower temperature. Compared to common coatings, thermochromic coatings exhibit 13–20 °C lower temperatures, except from yellow coating whose temperature difference is 5.6 °C (Fig. 7). Mean maximum daily surface temperatures until mid-September are 9.5–16.5 °C lower for thermochromic coatings compared to cool and 13.5–23 °C lower for thermochromic coatings compared to common, except from yellow ($\Delta T_{max(cool-thermo)} = 2.1$ °C, $\Delta T_{max(common-thermo)} = 4.5$ °C, respectively).

Nocturnal temperature differences between thermochromic, cool and common coatings are not significally important. This is explained by the study of the optical properties of the coatings discussed in Section 5.3.

Fig. 8 represents mean daily surface temperature rise of the green coatings in August in comparison with air temperature. Common, cool and thermochromic coatings without TiO_2 present higher temperature rise than the corresponding with TiO_2. In all cases the thermochromic coatings demonstrate lower temperature rise than cool and common. Negative values show that from late evening until early morning hours the air temperature is higher than the surface temperature of the tiles due to radiant cooling.

5. Comparative analysis of the optical performance of thermochromic coatings

5.1. Measurement of the spectral reflectance

Coatings were applied on rectangular aluminium plates of 8 cm × 8 cm. Spectral reflectance of thermochromic

Please cite this article in press as: Karlessi, T. et al., Development and testing of thermochromic coatings for buildings ..., Sol. Energy (2008), doi:10.1016/j.solener.2008.10.005

Table 2
Mean daily, mean maximum daily and mean nocturnal surface temperatures (°C) for thermochromic, cool and common coatings in August and September.

	Thermochromic		Cool		Common	
	With TiO_2	Without TiO_2	With TiO_2	Without TiO_2	Light	Dark
Mean daily surface temperature (°C) in August						
Green	33.2	36.0	40.9	43.8	44.6	48.5
Yellow	32.2	32.5	34.4	35.3	36.4	
Brown	31.0		40.2		42.3	
Black	37.6	38.4	44.6	45.2		47.5
Blue	33.1	37.4	38.7	42.4	39.0	43.9
Grey	34.1	35.5	40.4	44.4	45.1	
Mean maximum daily surface temperature (°C) in August						
Green	44.2	49.5	57.0	61.1	63.6	69.8
Yellow	42.5	43.8	44.0	46.7	49.3	
Brown	40.2		54.9		59.2	
Black	50.3	51.5	63.8	64.4		68.0
Blue	42.7	49.6	52.3	59.2	52.8	62.6
Grey	44.3	46.7	56.1	63.0	64.3	
Mean nocturnal surface temperature (°C) in August						
Green	18.0	17.8	20.2	21.6	20.2	20.7
Yellow	18.5	18.0	17.6	20.5	20.2	
Brown	18.6		21.0		20.6	
Black	21.3	21.1	20.4	20.6		21.1
Blue	20.0	20.6	20.7	20.5	20.9	20.2
Grey	21.0	20.5	20.2	20.8	20.3	
Mean daily surface temperature (°C) in September						
Green	26.1	28.6	34.0	37.9	38.1	42.3
Yellow	24.9	26.2	28.1	28.6	29.8	
Brown	23.8		34.2		35.9	
Black	30.9	31.6	38.8	39.2		41.0
Blue	26.1	31.4	32.2	35.7	32.8	37.7
Grey	26.6	29.0	32.9	37.4	37.9	
Mean maximum daily surface temperature (°C) in September						
Green	38.7	44.0	52.7	59.3	60.6	67.0
Yellow	36.4	39.7	43.0	41.8	44.2	
Brown	34.3		51.7		55.8	
Black	45.6	46.6	61.3	61.9		64.7
Blue	37.2	45.9	48.1	55.5	49.0	59.3
Grey	37.9	42.3	51.8	58.8	59.3	
Mean nocturnal surface temperature (°C) in September						
Green	12.2	11.6	14.1	15.0	13.9	15.1
Yellow	12.6	11.8	12.0	14.7	14.7	
Brown	12.4		14.9		14.5	
Black	15.3	15.3	14.4	14.4		15.0
Blue	14.2	14.9	14.7	14.3	15.0	14.3
Grey	15.0	14.5	12.7	14.7	14.6	

coatings was measured for the colored and the colorless state. The thermochromic plates were left to dry indoors. The set point temperature of the air-conditioned indoor space was 23 °C. A thermocouple connected to the data logger system was attached to the plate's surface during the measurement and indicated that the temperature ranged from 18 to 20 °C and the coating was fully colored. Then the thermochromic samples were exposed to outdoor conditions and their temperature was observed by the use of thermocouples. The spectral measurements were carried out at the first day of outdoor exposure when their temperature was 45 °C and they were completely decolorized. A heating device was used to maintain the samples temperature at approximately 45 °C during 3.5 min of each measurement. The results from the spectrophotometric measurements of the samples are presented in Fig. 9. In the visible range, the spectral curves of the thermochromic coating in its colored state and the corresponding cool and common coating coincide, meaning that they are of the same color. Small color differences that are depicted at the spectral curves are observed for the yellow coatings without TiO_2 and the grey coatings. Reflectance curves in the visible range of black, grey and yellow thermochromic coatings with TiO_2 at their colorless state indicate that at

Please cite this article in press as: Karlessi, T. et al., Development and testing of thermochromic coatings for buildings ..., Sol. Energy (2008), doi:10.1016/j.solener.2008.10.005

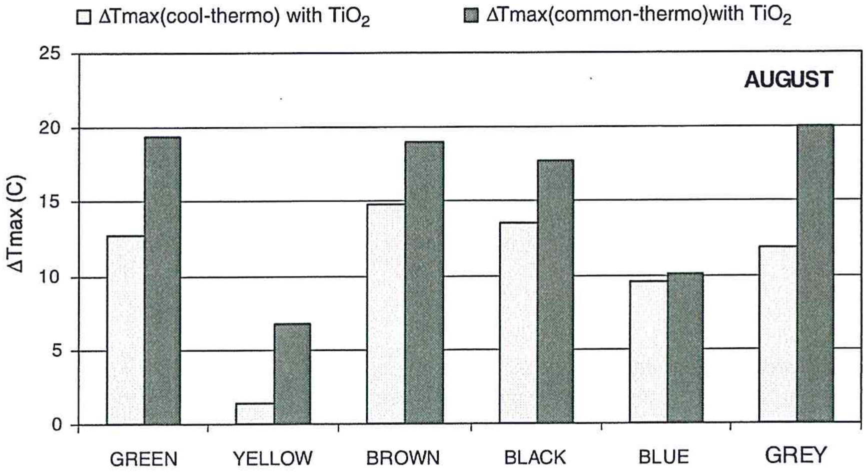

Fig. 6. Maximum surface temperature difference (ΔT_{max}) between thermochromic, cool and common coating with TiO_2 in August.

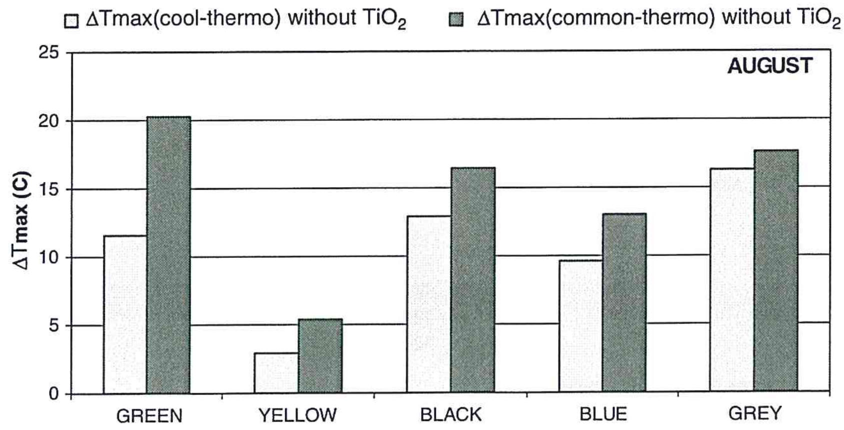

Fig. 7. Maximum surface temperature difference (ΔT_{max}) between thermochromic, cool and common coating without TiO_2 in August.

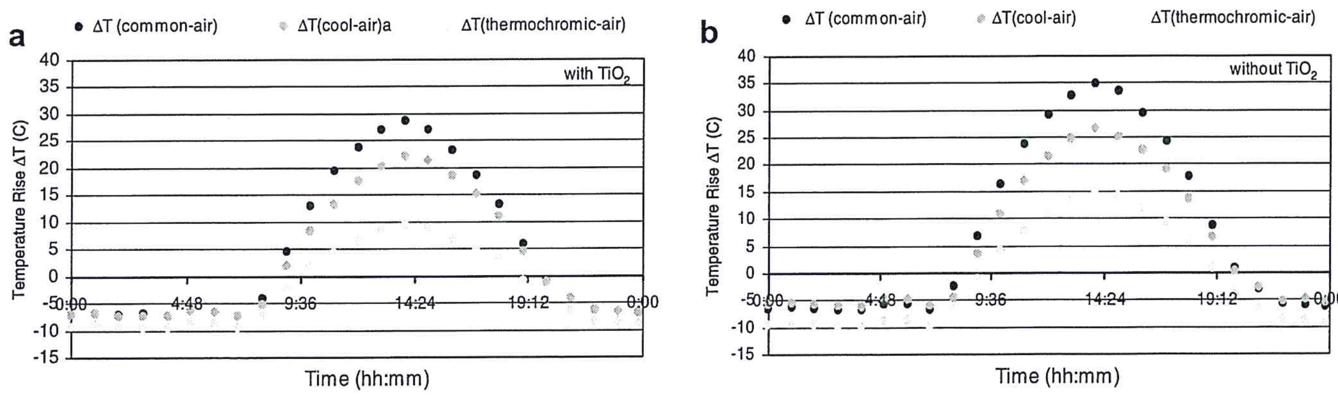

Fig. 8. Mean daily temperature rise of green colored thermochromic, cool and common coatings with TiO_2 (a) and without TiO_2 (b) in August compared to air temperature.

high temperatures coatings did not become completely white.

All coatings present very strong absorption in the near-ultraviolet range of the spectrum.

All thermochromic coatings are highly reflective in the near infrared (NIR). The reflectance curves of each color in the colored and the colorless state match as near infrared properties are mainly influenced by the pigments (Brady and Wake, 1992). The comparison between reflectance curves of thermochromic coatings at their colored phase (below the transition temperature of 30 °C) and their colorless phase (above the transition temperature of 30 °C) indi-

Please cite this article in press as: Karlessi, T. et al., Development and testing of thermochromic coatings for buildings ..., Sol. Energy (2008), doi:10.1016/j.solener.2008.10.005

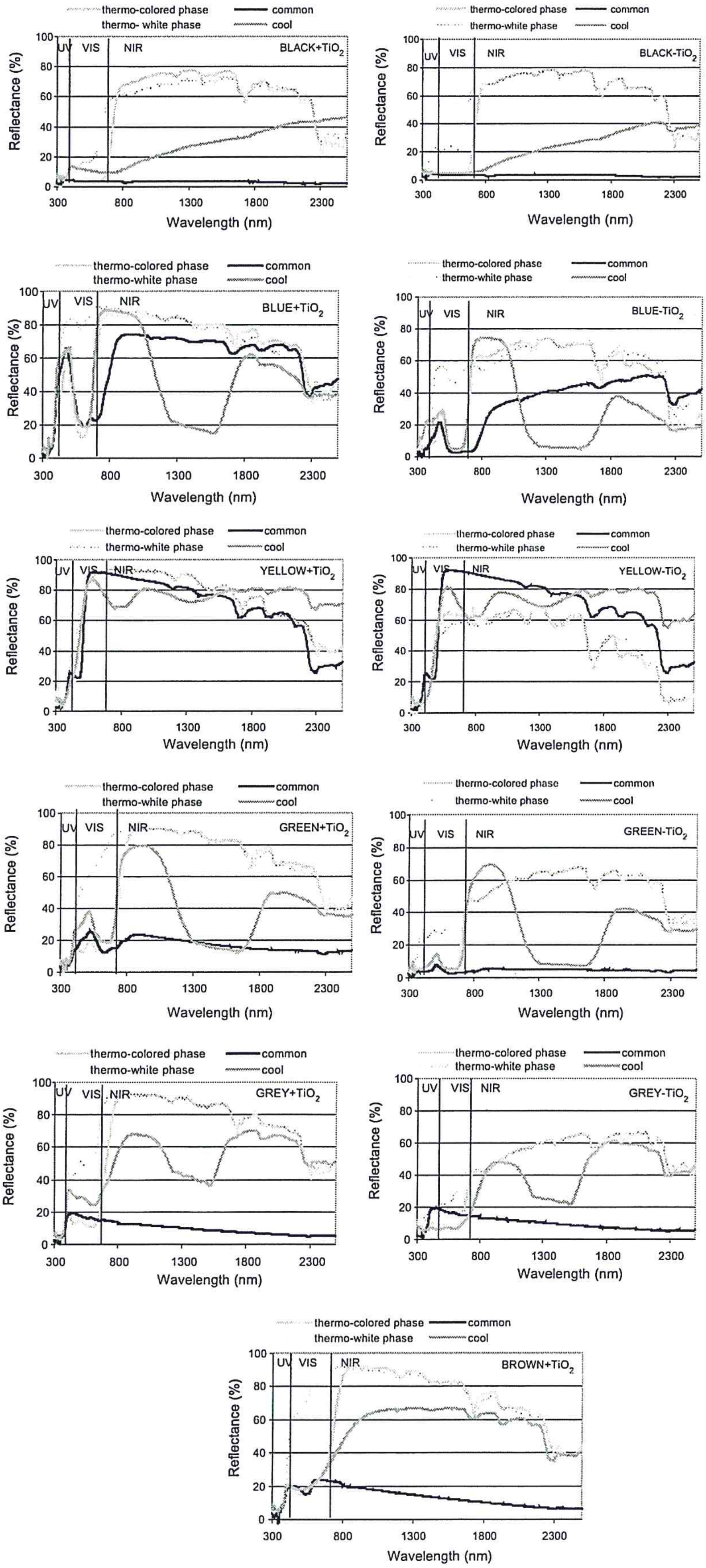

Fig. 9. Spectral reflectance of thermochromic, cool and common coatings of the same color.

cate that thermochromic building coatings can absorb solar energy at lower temperatures and reduce the absorption at higher temperatures.

5.2. Calculation of the solar reflectance

Data of the spectral measurements were used for the calculation of the solar reflectance of each sample. The calculation was performed by the weighted averaging method, using a standard solar spectrum as the weighting function. The spectrum employed is the one provided by ASTM (ASTM E903-96; ASTM G159-98). Table 3 presents the values of solar reflectance (SR) for each sample. Thermochromic coatings at both colored and colorless phase present higher solar reflectance values than cool and common color-matched coatings, according with lower temperatures that thermochromic coatings exhibit. Thermochromic samples with TiO_2, being light colored, present higher values of solar reflectance than the samples without TiO_2. The same applies to the colorless phase, where the coatings with TiO_2 become white, while the coatings without TiO_2 become translucent. Change in solar reflectance is also presented in Table 3. As also shown in Fig. 10, thermochromic coatings are more reflective in higher temperatures (colorless state) and more absorptive in lower temperatures (colored state). Best performing thermochromic coating considering its changing phase is green with TiO_2 which presents 0.22 change in solar reflectance between the colored and colorless phase, while for the yellow coating the change is only 0.03. Greatest differences of solar reflectance among thermochromic coatings at their colored state and their color-matched cool and common coatings are exhibited for black color. It is noticed that higher differences occur to dark colored coatings.

Table 3
Solar reflectance and change in solar reflectance of thermochromic, cool and common coatings.

Solar reflectance (SR)		Thermochromic		Change in SR	Cool	Change in SR	Common	Change in SR
		Colored phase	Colorless phase	SR(colorless–color)		SR(thermocolored–cool)		SR(thermocolored–common)
Green	With TiO_2	0.51	0.73	0.22	0.41	0.10	0.18	0.33
	Without TiO_2	0.33	0.45	0.12	0.27	0.06	0.04	0.29
Yellow	With TiO_2	0.78	0.81	0.03	0.73	0.05	0.64	0.14
	Without TiO_2	0.70	0.73	0.03	0.69	0.01	0.64	0.06
Brown	With TiO_2	0.55	0.76	0.21	0.41	0.14	0.18	0.37
Black	With TiO_2	0.40	0.53	0.13	0.17	0.23	0.03	0.37
	Without TiO_2	0.40	0.47	0.07	0.12	0.28	0.03	0.37
Blue	With TiO_2	0.59	0.71	0.12	0.53	0.06	0.51	0.08
	Without TiO_2	0.41	0.54	0.13	0.32	0.09	0.21	0.20
Grey	With TiO_2	0.55	0.73	0.18	0.44	0.11	0.13	0.42
	Without TiO_2	0.34	0.40	0.06	0.25	0.09	0.13	0.21

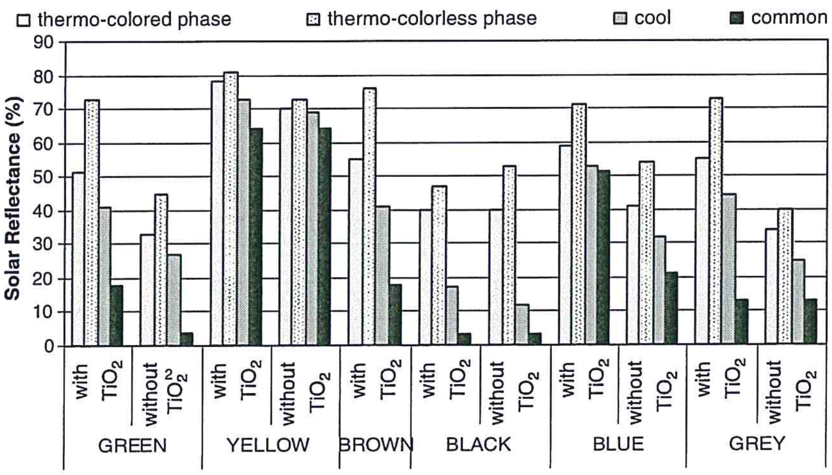

Fig. 10. Solar reflectance (%) of studied coatings.

Please cite this article in press as: Karlessi, T. et al., Development and testing of thermochromic coatings for buildings ..., Sol. Energy (2008), doi:10.1016/j.solener.2008.10.005

Table 4
Infrared emittance values of thermochromic, cool and common coatings.

Emittance		Thermochromic		Cool	Common
		Colored phase	Colorless phase		
Green	With TiO_2	0.90	0.88	0.87	0.91
	Without TiO_2	0.91	0.90	0.88	0.91
Yellow	With TiO_2	0.88	0.91	0.83	0.91
	Without TiO_2	0.90	0.87	0.84	0.91
Brown	With TiO_2	0.91	0.91	0.86	0.91
Black	With TiO_2	0.90	0.91	0.84	0.91
	Without TiO_2	0.92	0.88	0.87	0.91
Blue	With TiO_2	0.89	0.86	0.86	0.90
	Without TiO_2	0.90	0.86	0.87	0.90
Grey	With TiO_2	0.90	0.88	0.87	0.91
	Without TiO_2	0.89	0.89	0.88	0.91

5.3. Measurement of the infrared emittance

The values of infrared emittance of the coatings are presented in Table 4. Infrared emittance of the thermochromic coatings was measured at their colored and at their colorless phase. The total thermal emittance of all samples was determined in comparison with high and low emittance standard materials. The results indicate that infrared emittance of the samples ranges from 0.83 to 0.92 and that there is no significant difference between the values of thermochromic, cool and common coatings. Small variations in the emittance values explain the small variations in the mean nocturnal temperature values since infrared emittance is the predominant factor controlling the surface temperature during the night where solar radiation is absent.

6. Change in the spectral characteristics of the thermochromic coatings during a 10-day period

A test of the thermochromic samples was performed in order to investigate color degradation and impact of solar radiation on the thermochromic effect.

The thermochromic coatings were applied on rectangular aluminium plates of 8 × 8 cm, as shown in Fig. 1.

The samples were exposed to solar radiation for a 10-day period and daily measurements of the spectral reflectance of thermochromic coatings in their colored and colorless state were carried out. The measurements of the samples in their colored state took place in early morning hours when the samples were fully colored and their surface temperature was 20 °C, while the measurements in the colorless state took place around 15:00 pm, when their surface temperature was approximately 45 °C.

In Table 5 and Fig. 11 where calculated solar reflectance values are demonstrated, it can be noticed that reflectance values increase for the colored phase of thermochromic coatings from 1st to 10th day, while values decrease for the colorless phase. In agreement with these results, the tone of the colored phase lightens and the tone of the colorless phase darkens. This is clearly depicted in the visible part of the reflectance curves at Fig. 12. Spectral reflectance curves (Fig. 12) indicate that for the testing period there was no significant impact on the reflectance in the near infrared.

The greatest difference of solar reflectance values for the colored phase is noticed for the grey thermochromic coating without TiO_2 which exhibited an increase in solar reflectance by 28%, while the lowest difference of 2% is noticed for the yellow coating without TiO_2. At the colorless phase, solar reflectance is decreased by 5% for the yel-

Table 5
Daily values of solar reflectance (SR) for thermochromic sample and solar reflectance difference ΔSR for 1st and 10th day.

Solar reflectance	SR	Day 1	Day 5	Day 10	ΔSR (D10–D1)
Black + TiO_2	Colored phase	0.40	0.45	0.43	0.03
	Colorless phase	0.47	0.48	0.46	−0.01
Black − TiO_2	Colored phase	0.39	0.41	0.44	0.05
	Colorless phase	0.46	0.46	0.45	−0.01
Blue + TiO_2	Colored phase	0.61	0.70	0.70	0.09
	Colorless phase	0.79	0.81	0.77	−0.02
Blue − TiO_2	Colored phase	0.40	0.43	0.44	0.04
	Colorless phase	0.48	0.46	0.46	−0.02
Green + TiO_2	Colored phase	0.53	0.63	0.64	0.11
	Colorless phase	0.75	0.75	0.73	−0.02
Green − TiO_2	Colored phase	0.35	0.40	0.41	0.06
	Colorless phase	0.44	0.43	0.42	−0.02
Yellow + TiO_2	Colored phase	0.78	0.79	0.74	−0.04
	Colorless phase	0.80	0.78	0.68	−0.12
Yellow − TiO_2	Colored phase	0.54	0.57	0.53	−0.01
	Colorless phase	0.50	0.51	0.51	0.01
Grey + TiO_2	Colored phase	0.59	0.71	0.71	0.12
	Colorless phase	0.72	0.75	0.75	0.03
Grey − TiO_2	Colored phase	0.35	0.46	0.45	0.10
	Colorless phase	0.40	0.46	0.44	0.04
Brown + TiO_2	Colored phase	0.57	0.65	0.66	0.09
	Colorless phase	0.78	0.77	0.75	−0.03

Please cite this article in press as: Karlessi, T. et al., Development and testing of thermochromic coatings for buildings ..., Sol. Energy (2008), doi:10.1016/j.solener.2008.10.005

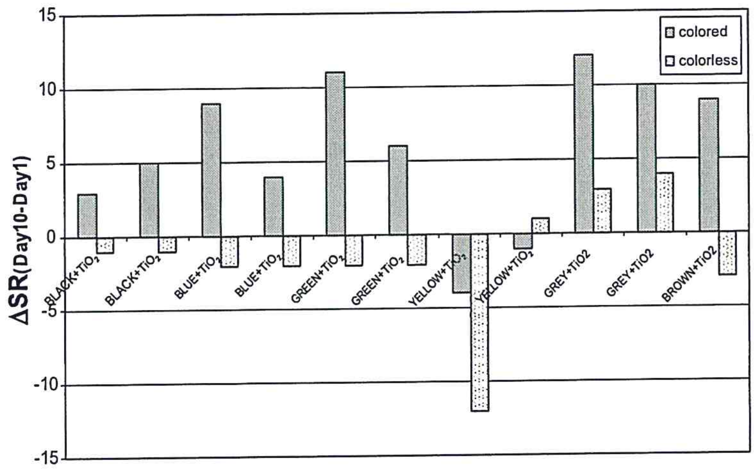

Fig. 11. Solar reflectance difference (ΔSR) between 1st and 10th day for thermochromic coatings.

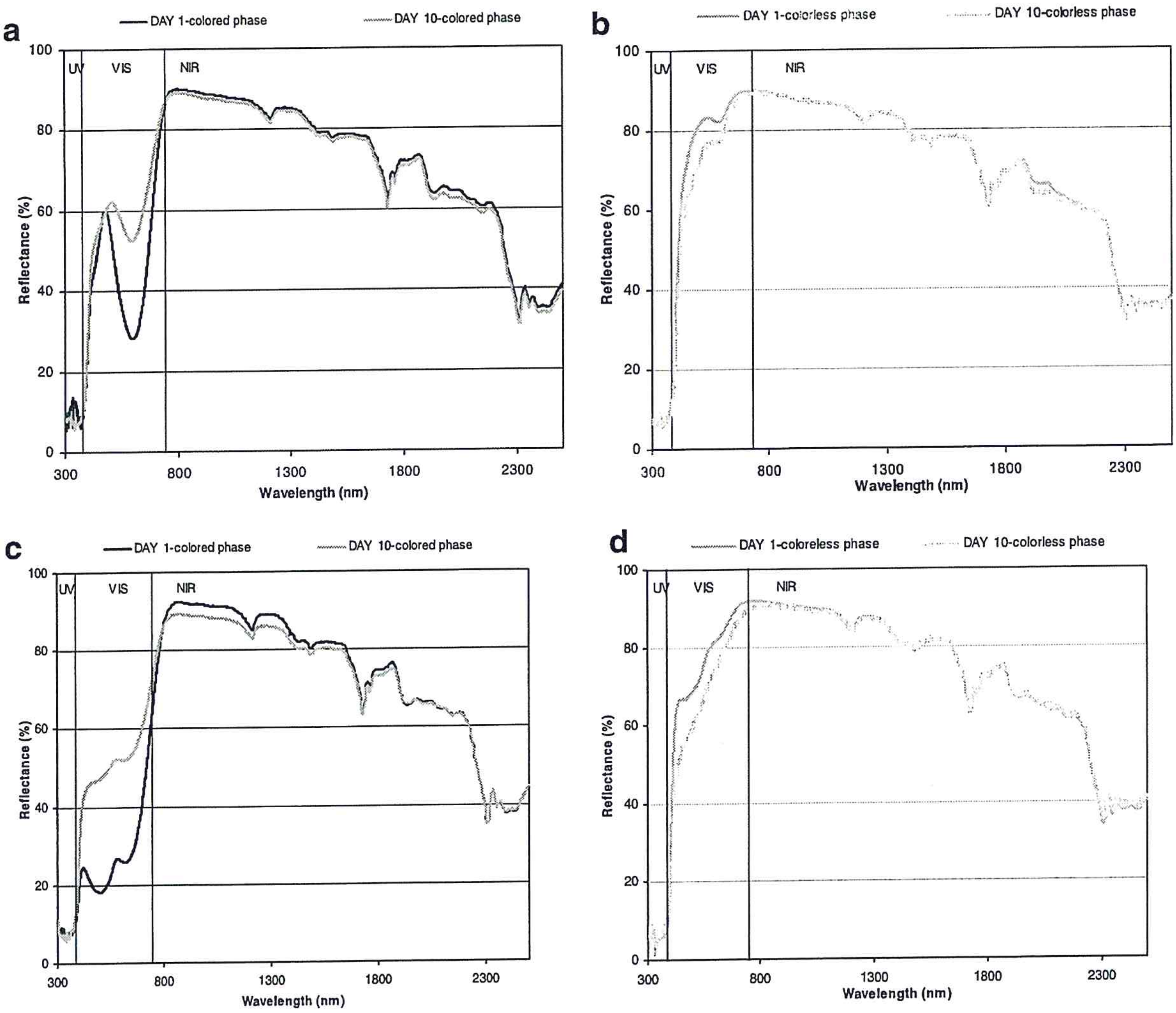

Fig. 12. Spectral curves of thermochromic coatings for the 10-day testing period: blue with TiO_2 (a and b) and brown with TiO_2 (c and d). No significant change in the reflectance in the near infrared has been observed.

low coating with TiO_2 and by 2% for the black coatings. A general remark is that the degradation of color and solar reflectance is more intense for the colored than the colorless phase. Increase of solar reflectance is not observed though for the colored phase of yellow coatings and decrease is not observed for the colorless phase of grey coatings. Further research to stabilize the optical properties of the materials is on going.

7. Conclusions

Eleven thermochromic coatings were developed by using thermochromic pigments into an appropriate binder system. The color-changing temperature was 30 °C. The same binder system was used for the production of highly reflective (cool) and common coatings, in order to investigate and compare the thermal and optical characteristics of color-matched thermochromic, cool and common coatings. Thermochromic samples were divided in two groups: group without TiO_2 and with TiO_2 so as to investigate the properties of thermochromic pigments without the interaction with other substances and increase the hiding power of the coating, respectively. In order to obtain comparative results a group with TiO_2 and a group without TiO_2 were also produced for the cool coatings. The results demonstrated that during the experimental period (August–mid-September 2007), surface temperatures of thermochromic samples were lower than the temperatures of color-matched cool and common. Mean daily surface temperatures ranged from 23.8 to 38.4 °C for the thermochromic samples, from 28.1 to 44.6 °C for the cool and from 29.8 to 48.5 °C for the common samples. Thermochromic coatings with TiO_2 (lighter tones) showed lower temperatures than samples without TiO_2 (darker tones). Spectral measurements revealed that all thermochromic coatings are highly reflective in the near infrared. At higher temperatures, being colorless, they reflect solar energy, while at lower temperatures, being colored, they absorb solar energy. The maximum solar reflectance increase from colored to colorless phase was 43%. Solar reflectance values were higher for thermochromic coatings at the colored phase compared to cool and common of the same color. Measurement of the infrared emittance did not indicate significant differences between the three types of coatings. Degradation of spectral characteristics of the thermochromic samples was also investigated and it was noticed that there was a high impact of solar radiation on thermochromism. During the 10-day experimental period, the colored phase faded and solar reflectance was increased, while the tone of the colorless phase became darker and solar reflectance was decreased.

From this study it is concluded that thermochromic systems can function as energy saving systems. For high temperatures, during summertime thermochromic coatings have the ability to reflect solar energy, reducing the surface's temperature, while in wintertime absorb solar energy, increasing the surface's temperature as reversible color change takes place. Applied thus on external building surfaces, they have the potential for the reduction of heating and cooling loads, contributing to the reduction of urban temperatures, fight heat island and reduce air pollution.

Further research is required in order to improve the thermochromic coating's performance by preventing photodegradation with the use of photostabilizers such as UV-absorbers, etc.

References

Aitken, D., Burkinshaw, S.M., Griffiths, J., Towns, A.D., 1996. Textile applications of thermochromic systems. Journal of Review of Progress in Coloration 26, 1–8.

Akbari, H., Bretz, S., Taha, H., Kurn, D., Hanford, J., 1997. Peak power and cooling energy savings of high albedo roofs. Journal of Energy and Buildings – Special Issue on Urban Heat Islands and Cool Communities, 25(2), 117–126.

Akbari, H., Davis, S., Dorsano, S., Huang, J., Winert, S., 1992. Cooling our Communities – A Guidebook on Tree Planting and White Colored Surfacing. US Environmental Protection Agency, Office of Policy Analysis, Climate Change Division.

Akbari, H., Konopacki, S., Pomerantz, M., 1999. Cooling energy savings potential of reflective roofs for residential and commercial buildings in the United States. Journal of Energy 24, 391–407.

ASTM Standard E903-96. Standard Test Method for Solar Absorptance, Reflectance and Transmittance of Materials Using Integrating Spheres.

ASTM Standard G159-98. Standard Tables for References Solar Spectral Irradiance at Air Mass 1.5: Direct Normal and Hemispherical for a 37° Tilted Surface.

Azari, S., Bierman, J., 2005. System and method for energy-conserving roofing. United States Patent No. 0064175.

Bamfield, P., 2001. Chromic phenomena, technological applications of color chemistry. Royal Society of Chemistry, 33–41.

Berdahl, P., Bretz, S., 1997. Preliminary survey of the solar reflectance of cool roofing materials. Journal of Energy and Buildings 25, 149–158.

Berdahl, P., Akbari, H., Levinson, R., Miller, W., 2008. Weathering of roofing materials – an overview. Journal of Construction and Building Materials. 22 (4), 423–433.

Brady, R.F., Wake, L.V., 1992. Principles and formulations for organic coatings with tailored infrared properties. Journal of Progress in Organic Coatings 20, 1–20.

Bretz, S., Akbari, H., 1997. Long-term performance of high albedo roof coatings. Journal Energy and Buildings 25, 159–167.

Bretz, S., Akbari, H., Rosenfeld, A., 1997. Practical issues for using solar-reflective materials to mitigate urban heat islands. Journal of Atmospheric Environment 32, 95–101.

Color Change Corporation, 2007. <www.colorchange.com>.

Cornelius Group PLC (Matsui International Co.), 2007. <www.cornelius.co.uk>.

Cremer, M., 1981. Evaluation of hiding power of organic coatings-measurement, methods and other limitations. Progress in Organic Coatings 9, 241–279.

Fujita, K., Senga, K., 2002. Thermochromic microencapsulated pigments. United States Patent No. 6494950.

Fujita, K., Ono, Y., Shibahashi, Y., 1997. Method for improving lightfastness of reversible thermochromic compositions at the time of color extinguishment. United States Patent No. 5879438.

Geros, V., Santamouris, M., Karatasou, S., Tsangrassoulis, A., Papanikolaou, N., 2005. On the cooling potential of night ventilation techniques in the urban environment. Journal of Energy and Buildings 37, 243–257.

Hassid, S., Santamouris, M., Papanikolaou, N., Linardi, A., Klitsikas, N., Georgakis, C., Assimakopoulos, D., 2000. The effect of the Athens heat island on air conditioning load. Journal of Energy and Buildings 32, 131–141.

Livada, I., Santamouris, M., Niachou, K., Papanikolaou, N., Mihalakakou, G., 2002. Determination of places in the great Athens area where the heat island effect is observed. Journal of Theoretical and Applied Climatology 71, 219–230.

Please cite this article in press as: Karlessi, T. et al., Development and testing of thermochromic coatings for buildings ..., Sol. Energy (2008), doi:10.1016/j.solener.2008.10.005

Ma, Y., Zhu, B., Wu, K., 2001. Preparation and solar reflectance spectra of chameleon-type building coatings. Journal of Solar Energy 70, 417–422.

Ma, Y., Zhang, X., Zhu, B., Wu, K., 2002. Research on reversible effects and mechanism between the energy-absorbing and energy-reflecting states of chameleon-type building coatings. Journal of Solar Energy 72, 511–520.

MacLaren, D., White, M.A., 2003a. Dye–developer interactions in the crystal violet lactone–lauryl gallate binary system: implications for thermochromism. Journal of Materials Chemistry 13, 1695–1700.

MacLaren, D., White, M.A., 2003b. Competition between dye–developer and solvent–developer interactions. Journal of Materials Chemistry 13, 1701–1704.

McNaught, A., Wilkinson, A., 1997. Compendium of Chemical Terminology. IUPAC, second ed. The Royal Society of Chemistry, Blackwell Science, Cambridge, UK.

Mihalakakou, P., Flokas, H., Santamouris, M., Helmis, C., 2002. Application of neural networks to the simulation of the heat island over Athens, Greece using synoptic types as a predictor. Journal of Applied Meteorology 41, 519–527.

Mihalakakou, G., Santamouris, M., Papanikolaou, N., Cartalis, C., Tsangrassoulis, A., 2004. Simulation of the urban heat island phenomenon in mediterranean climates. Journal of Pure and Applied Geophysics 161, 429–451.

Neves, R., 2001. Use of thermochromic black pigments on white textile or coating materials, to save energy in buildings or other closed spaces. Word Intellectual Property Organization, Patent No. 92633.

Novinson, T., 1996. Reversible thermochromic pigments. United States Patent No. 5480482.

Pospisil, J., Nespurec, S., 2000. Photostabilization of coatings. Mechanisms and performance. Journal of Progress in Polymer Science 25, 1261–1335.

Prado, R., Ferreira, 2005. Measurement of albedo and analysis of its influence the surface temperature of building roof materials. Journal of Energy and Buildings 37, 295–300.

Rosenfeld, A.H., Akbari, H., Pomerantz, M., Taha, H., Romm, J., 1996. Policies to reduce heat islands: magnitudes of benefits and incentives to achieve them. In: Proceedings of the 1996 ACEEE Summer Study on Energy Efficiency in Buildings, vol. 9.

Santamouris, M., 2001. Energy and Climate in the Urban Built Environment. James and James Science Publishers, London.

Santamouris, M., 2007. Heat Island Research in Europe. The State of the Art. Journal of Advances Building Energy Research, ABER.

Santamouris, M., Mihalakakou, G., Papanikolaou, N., Assimakopoulos, D., 1999. A neural network approach for modelling the heat island phenomenon in urban areas during the summer period. Geophysics Research Letters 26, 337–340.

Santamouris, M., Papanikolaou, N., Livada, I., Koronakis, I., Georgakis, C., Argiriou, A., Assimakopoulos, D., 2001. On the impact of urban climate to the energy consumption of buildings. Journal of Solar Energy 70, 201–216.

Santamouris, M., Adnot, J., Alvarez, S., Klitsikas, N., Orphelin, M., Lopes, C., Sanchez, F., 2004. Cooling the Cities. Eyrolees, Paris, France, ISBN: 2-911762-54-1.

Santamouris, M., Paraponiaris, K., Mihalakakou, G., 2007. Estimating the ecological footprint of the heat island effect over Athens, Greece. Journal of Climatic Change 80, 265–276.

Shibahashi, Y., Nakasuji, N., Kataota, T., Inagaki, H., Kito, T., 1984. Thermochromic materials. United States Patent No. 4425161.

Synnefa, A., Santamouris, M., Livada, I., 2006. A study of the thermal performance of reflective coatings for the urban environment. Journal of Solar Energy 80, 968–981.

Synnefa, A., Dandou, A., Santamouris, M., Tombrou, M., 2007a. An energy efficient solution to mitigate heat islands and reduce cooling energy loads. In: Braganca, L. (Ed.), Proceedings of Sustainable Buildings 2007, International Conference, Lisbon, Portugal, pp. 895–902.

Synnefa, A., Santamouris, M., Akbari, H., 2007b. Estimating the effect of using cool coatings on energy loads and thermal comfort in residential buildings in various climatic conditions. Journal of Energy and Buildings 39, 1167–1174.

Synnefa, A., Santamouris, M., Apostolakis, K., 2007c. On the development, optical properties and thermal performance of cool colored coatings for the urban environment. Journal of Solar Energy 81, 488–497.

Watts, D., Battista, L., Zunino, J., 2006. Smart coating system. United States Patent No. 0182160.

White, M.A., LeBlanc, M., 1999. Thermochromism in commercial products. Journal of Chemical Education 76, 1201–1205.

White, G., Zartman, D., Bonicamp, J., 2000. A serious look at changeable silly putty. Journal of Chemical Educator 5, 2–7.

Yoshikawa, K., Fukuo, H., Kuroda, J., 1986. Thermochromic compositions. United States Patent No. 4620941.

Please cite this article in press as: Karlessi, T. et al., Development and testing of thermochromic coatings for buildings ..., Sol. Energy (2008), doi:10.1016/j.solener.2008.10.005